The Cul3 ubiquitin ligase engages Insomniac as an adaptor to impact sleep and synaptic homeostasis

Qiuling Li[1], Kayla Y. Lim[1], Raad Altawell[3], Faith Verderose[3], Celine Dong[2], Joshua Martinez[2], Xiling Li[2], Dion Dickman[2], and Nicholas Stavropoulos[3,*]

[1]NYU Neuroscience Institute, Department of Neuroscience and Physiology, New York University School of Medicine, New York, NY 10016, USA

[2]Department of Neurobiology, University of Southern California, Los Angeles, CA 90089, USA

[3]Waksman Institute, Rutgers University, Piscataway, NJ 08854, USA

Keywords: Cullin-3, Inc, KCTD2, KCTD5, KCTD17, BTB, autism, schizophrenia, myoclonic dystonia

Running Title: Cul3 impacts sleep and synapses through Insomniac

[*]Correspondence: stavropoulos@waksman.rutgers.edu

Abstract

Mutations of the Cullin-3 (Cul3) E3 ubiquitin ligase are associated with autism and schizophrenia, neurological disorders characterized by sleep disturbances and altered synaptic function. Cul3 engages dozens of adaptor proteins to recruit hundreds of substrates for ubiquitination, but the adaptors that impact sleep and synapses remain ill-defined. Here we implicate Insomniac (Inc), a conserved protein required for normal sleep and synaptic homeostasis in *Drosophila*, as a Cul3 adaptor. Inc binds Cul3 in vivo, and mutations within the N-terminal BTB domain of Inc that weaken Inc-Cul3 associations impair Inc activity, indicating that Inc function requires binding to the Cul3 complex. Deletion of the conserved C-terminus of Inc does not alter Cul3 binding but abolishes Inc activity in the context of sleep and synaptic homeostasis, suggesting that the C-terminal domain of Inc is a substrate recruitment domain. Mutation of a conserved, disease-associated arginine in the Inc C-terminus also abolishes Inc function, suggesting that this residue is vital for recruiting Inc targets. Inc levels are negatively regulated by Cul3 in neurons, consistent with Inc degradation by autocatalytic ubiquitination, a hallmark of Cullin adaptors. These findings link Inc and Cul3 in vivo and indicate that Cul3-Inc complexes are essential for normal sleep and synaptic function. Furthermore, these results indicate that dysregulation of conserved substrates of Cul3-Inc complexes may contribute to altered sleep and synaptic function in autism and schizophrenia associated with *Cul3* mutations.

Author Summary

Cul3 is a highly conserved gene important for brain development and function. *Cul3* mutations are a risk factor for autism and schizophrenia, neurological disorders associated with disturbed sleep and changes in neuronal synapses. A key challenge in understanding how *Cul3* impacts brain function is elucidating the downstream molecular pathways. Cul3 is a ubiquitin ligase that assembles with dozens of adaptor proteins, which in turn recruit specific protein substrates for ubiquitination. Identifying and characterizing Cul3 adaptors in the nervous system is thus a critical step in understanding Cul3 function. Because Cul3 and its adaptors are conserved through evolution, simpler organisms including the fruit fly *Drosophila* provide powerful systems for identifying and characterizing Cul3 adaptors. We found that the Insomniac (Inc) protein has the properties of a Cul3 adaptor that impacts sleep and synaptic function in *Drosophila*. These results suggest that human proteins related to Inc may be relevant for changes in sleep and synaptic function in autism and schizophrenia associated with reduced Cul3 activity.

55 **Introduction**

56 The Cullin-3 (Cul3) E3 ubiquitin ligase is broadly expressed in the brain and is an
57 important regulator of nervous system development and function. In humans, *Cul3* mutations are
58 linked to autism, its associated sleep disturbances, and to schizophrenia [1–7]. Mice bearing *Cul3*
59 mutations exhibit alterations in neurogenesis, dendritic development, synaptic transmission, and
60 glutamate receptor levels, as well as social deficits relevant to autism spectrum disorder [8–14].
61 *Cul3* is highly conserved, and reduced activity of *Cul3* in worms and flies causes similar
62 phenotypes within the nervous system, including perturbations in neuronal morphogenesis,
63 glutamate receptor abundance, synaptic homeostasis, and sleep [15–20].

64 A key challenge in understanding how *Cul3* impacts brain function is elucidating the
65 downstream molecular pathways. Cul3 assembles in a modular fashion with dozens of BTB-
66 domain adaptor proteins that recruit substrates to Cul3 complexes for ubiquitination [21–25].
67 Which among the known and putative adaptors of Cul3 contribute to its phenotypes—including
68 sleep disturbances and altered synaptic function—remains largely unknown. Though several Cul3
69 adaptors have been characterized in neurons [16,26–32], many known and putative Cul3 adaptors
70 have yet to be assessed.

71 *insomniac* (*inc*) encodes a conserved BTB-domain protein that is hypothesized to serve as
72 a Cul3 adaptor [17,18,33]. *inc* null mutations reduce sleep duration and consolidation in
73 *Drosophila* and impair synaptic homeostasis, phenotypes that are recapitulated by reduced *Cul3*
74 activity [17,18,20]. Inc can bind Cul3 when overexpressed in cultured cells [17,18,33], but whether
75 these interactions occur in vivo or are required for the activity of Inc is unknown. Notably, some
76 BTB-domain proteins associate with Cul3 but are unlikely to serve as adaptors [34]. Functional
77 analysis has been essential to distinguish Cul3 adaptors within the BTB superfamily, which also
78 includes $GABA_B$ receptor subunits, potassium channels, and transcriptional regulators [35,36]. In

79 the absence of evidence linking Inc and Cul3 in vivo, the role of Inc as a Cul3 adaptor has remained
80 speculative.

81 Here we implicate Inc as a Cul3 adaptor, using biochemical, behavioral, and
82 electrophysiological studies of Inc mutants. Critically, Inc binds Cul3 in vivo and Inc activity
83 requires the assembly of Inc-Cul3 complexes. Inc function also requires its C-terminus, a
84 conserved domain dispensable for Cul3 associations but vital for Inc activity, consistent with the
85 properties of a substrate recruitment domain. Mutation of a conserved C-terminal arginine
86 abolishes Inc function, suggesting that this residue is vital for recruiting Inc targets. Mutation of
87 the same residue in the human Inc ortholog KCTD17 is associated with myoclonic dystonia [37],
88 consistent with a critical and evolutionarily conserved function for this residue in Inc orthologs.
89 Our results reveal that Cul3-Inc complexes impact sleep and synaptic function, and provide tools
90 to identify targets of Cul3, Inc, and Inc orthologs that impact normal brain function and
91 neurological disorders.

92 **Results**

93 **The Inc BTB domain mediates Cul3 binding and Inc multimerization**

94 Cul3 adaptors have a modular functional organization, with BTB domains that self-
95 associate and bind Cul3, and distal domains that recruit substrates [21–24]. Inc has two conserved
96 domains, an N-terminal BTB domain and a C-terminal domain unique to Inc and its orthologs
97 [17,38,39] (Fig 1A and S1A Fig). To determine whether Inc has the properties of a Cul3 adaptor,
98 we generated progressive N- and C-terminal deletions of Inc (Fig 1A) and assessed whether these
99 derivatives could bind Inc and Cul3, by expressing epitope-tagged forms of these proteins in
100 *Drosophila* S2 cells and performing co-immunoprecipitations.

101 Deleting Inc residues preceding the BTB domain (Inc^{22-211}) did not alter Inc stability or
102 Inc-Cul3 interactions (Fig 1B and S2 Fig), indicating that the N-terminus of Inc is dispensable for
103 Cul3 binding. In contrast, removing part of the BTB domain (Inc^{31-211}) or the entire BTB domain
104 ($Inc^{124-211}$) significantly destabilized Inc (S2 Fig), and low steady-state levels of these proteins
105 precluded conclusions about their ability to bind Cul3. Inc proteins lacking 25 C-terminal residues
106 (Inc^{1-186}) or all residues following the BTB domain (Inc^{1-123}) were stable and associated with Cul3
107 similarly to full-length Inc. An Inc mutant lacking most of the Inc C-terminal domain (Inc^{1-156})
108 was stable and interacted with Cul3 more strongly than wild-type Inc and other Inc deletions (S3A
109 Fig). Thus, the Inc C-terminus is dispensable for interaction with Cul3. The Inc BTB domain alone
110 (Inc^{22-123}) was sufficient to bind Cul3, albeit more weakly than wild-type Inc (S3B Fig); because
111 deleting the same N-terminal residues from full length Inc slightly weakened Cul3 binding (Fig
112 1B; Inc^{22-211} versus Inc^{1-211}), these results suggest that Inc N-terminal residues stabilize Cul3
113 interactions mediated chiefly by the Inc BTB domain.

114 Cul3 adaptors homomultimerize through their BTB domains, and adaptor-mediated
115 oligomerization of Cul3 complexes can enhance substrate ubiquitination [40]. We therefore

116 assessed whether Inc self-association is mediated by its BTB domain. N-terminal truncations that
117 preserve the Inc BTB domain (Inc^{22-211}) did not alter Inc-Inc associations (Fig 1C). Similarly, Inc
118 proteins truncated C-terminally (Inc^{1-186}, Inc^{1-156}, and Inc^{1-123}) associated with Inc normally,
119 indicating that the Inc C-terminus is dispensable for Inc multimerization (Fig 1C). The Inc BTB
120 domain (Inc^{22-123}) alone was sufficient to bind Inc (Fig 1C). Thus, the Inc BTB domain is sufficient
121 to mediate both Inc multimerization and Cul3 binding, as expected of a Cul3 adaptor.
122

123 **Inc point mutants define a surface of the Inc BTB domain that binds Cul3**

124 To determine whether Inc function in vivo requires binding to Cul3 and Inc
125 homomultimerization, we sought to identify Inc point mutants that selectively perturb Inc-Cul3
126 and Inc-Inc interactions. Our mutagenesis of Inc was informed by the structures of homodimeric
127 BTB-MATH and BTB-BACK-Kelch adaptors bound to Cul3 [40–42], and by the structure of
128 KCTD5, a human Inc ortholog that forms homopentamers [39]. Homology modeling and light
129 scattering measurements suggest that Inc forms a homopentamer similar to that of KCTD5 [43,44].
130 We selected eight conserved residues in the Inc BTB domain whose equivalents in KCTD5 reside
131 on a surface suggested to bind Cul3 [43,45] (S1A Fig). We mutated these residues to alanine
132 (F47A, D57A, D61A, F105A, N107A), to oppositely charged residues (R50E, E104K), or altered
133 their hydrophobicity (Y106F), and assessed the effects on Inc-Cul3 and Inc-Inc binding. Most of
134 these mutants did not alter Inc-Cul3 or Inc-Inc interactions, while one mutant (R50E) impaired
135 both associations (S1 Table). Two mutants, F47A and F105A (Fig 2A), weakened interactions
136 with Cul3 (Fig 2B) but did not significantly affect Inc self-association or stability (Fig 2C and S4
137 Fig). Similarly, an F47A/F105A double mutant was stable and selectively impaired Cul3 binding
138 (Fig 2B and 2C and S4 Fig). The analogous phenylalanines in KCTD5 cluster near the interface
139 of adjacent subunits, defining a surface for Cul3 binding (S1B Fig).

140 To identify Inc mutants that impair its multimerization, we selected seven conserved
141 residues whose equivalents in KCTD5 engage in polar and charged interactions between adjacent
142 subunits [39] (S1A and S1C Fig). Mutating these residues individually or in double mutant
143 combinations to alanine (T36A, D71A, D73A, N82A) or to oppositely charged residues (R85E,
144 K88D, E101K) did not significantly alter Inc self-association (S2 Table). A triple mutant
145 (T36A/D71A/R85E) predicted to disrupt interactions of Inc subunits with both flanking neighbors
146 in a putative Inc homopentamer exhibited significantly reduced stability (S4 Fig and S2 Table),
147 precluding conclusions about its ability to multimerize and bind Cul3. Because this triple mutant
148 was also unstable when expressed in vivo, we focused further analysis on Inc mutants that
149 selectively perturb Cul3 interactions.
150
151 **Inc function in vivo requires the assembly of Inc-Cul3 complexes**
152 To determine whether Inc impacts sleep as a Cul3 adaptor, we assessed whether Inc
153 mutants that weaken Cul3 binding impair Inc activity in vivo. We generated UAS transgenes
154 expressing 3×FLAG-tagged Inc, Inc^{F47A}, Inc^{F105A}, and $Inc^{F47A/F105A}$, integrating them at the same
155 genomic site to compare their activity. When expressed with *inc-Gal4*, a driver that rescues *inc*
156 mutants when used to restore *inc* expression [17,33], Inc and Inc mutants were similarly stable in
157 both inc^{1} and inc^{+} animals (Fig 3A and S5 Fig). Because Inc mutants deficient for Cul3 binding
158 might sequester substrates and function as dominant negatives, we tested whether these mutants
159 could alter sleep when expressed in neurons. Neuronal expression of Inc^{F47A}, Inc^{F105A}, or
160 $Inc^{F47A/F105A}$ did not alter sleep (S6A Fig), in contrast to neuronal *inc* RNAi [17,18]. Similarly,
161 expression of these mutants using *inc-Gal4* did not perturb sleep (S6D Fig). Thus, these Inc
162 mutants do not antagonize endogenous Inc, possibly because they retain some ability to bind Cul3
163 (Fig 2B). Finally, we tested whether Inc function in vivo requires the assembly of Inc-Cul3

164 complexes. If so, Inc mutants that weaken Cul3 binding should impair *inc* rescue. Whereas wild-
165 type Inc expressed with *inc-Gal4* fully rescued daily sleep duration in *inc*^{1} mutants, Inc^{F47A}
166 provided only a partial rescue, and Inc^{F105A} and Inc$^{F47A/F105A}$ failed to restore a significant amount
167 of sleep (Fig 3B and 3C), indicating that Inc activity requires binding to the Cul3 complex. For
168 other sleep parameters, rescue was more strongly impaired for Inc^{F105A} and Inc$^{F47A/F105A}$ than for
169 Inc^{F47A} (S7A–D Fig), suggesting that F105 is particularly critical for Cul3 binding in vivo. All
170 rescuing activity of UAS transgenes was Gal4-dependent, as indicated by the short sleep of *inc*^{1}
171 mutants bearing only UAS transgenes (S8 Fig). Collectively, these results indicate that Inc function
172 in vivo requires the assembly of Inc-Cul3 complexes and that their disruption inhibits sleep.
173

174 **The Inc C-terminus is vital for Inc activity in vivo and has the properties of a substrate**
175 **recruitment domain**

176 Although the Inc C-terminus is dispensable for Inc-Inc and Inc-Cul3 associations (Fig 1B
177 and 1C), its evolutionary conservation suggests a critical function. The modular structure of Cul3
178 adaptors suggests that if Inc serves as a Cul3 adaptor, its C-terminus would bind and recruit
179 substrates to Inc-Cul3 complexes. We therefore assessed the activity of C-terminally truncated Inc
180 mutants in vivo. 3×FLAG-tagged Inc$^{1-186}$, Inc$^{1-156}$, and Inc$^{1-123}$ were expressed at similar levels
181 under *inc-Gal4* control (Fig 4A), indicating that they are stable in vivo, as in cultured cells (Fig
182 1B and 1C). Expression of C-terminally truncated Inc mutants neuronally with *elav-Gal4* or with
183 *inc-Gal4* did not alter sleep, indicating that they do not inhibit endogenous *inc* function (S6B Fig
184 and S6D Fig). We next tested whether C-terminally truncated Inc proteins could restore sleep to
185 *inc* mutants. Wild-type Inc expressed with *inc-Gal4* fully rescued sleep in *inc*^{1} mutants (Fig 4B
186 and 4C). In contrast, C-terminal truncations of Inc curtailed or abolished Inc function. Inc$^{1-186}$
187 partially rescued *inc* mutants, while animals expressing Inc$^{1-156}$ or Inc$^{1-123}$ slept indistinguishably

188 from *inc* mutants, indicating that Inc^{1-156} and Inc^{1-123} lacked activity in vivo (Fig 4B and 4C and
189 S9A–D Fig). Thus, the Inc C-terminus is vital for Inc function. The ability of C-terminally
190 truncated Inc proteins to multimerize and bind Cul3 normally (Fig 1B and 1C) is consistent with
191 a modular function for the Inc C-terminus in recruiting targets that impact sleep.
192

193 **Inc-Cul3 binding and the Inc C-terminus are vital for Inc activity at synapses**

194 We next assessed whether Inc-Cul3 associations and the Inc C-terminus are required for
195 Inc function at synapses. At the larval neuromuscular junction, Inc is required for the homeostatic
196 upregulation of presynaptic neurotransmitter release caused by inhibition of postsynaptic
197 glutamate receptors [20]. Application of philanthotoxin, a glutamate receptor antagonist, reduces
198 the amplitude of spontaneous neurotransmission, while homeostatic upregulation of evoked
199 neurotransmission maintains synaptic strength in wild-type animals (Fig 5A and 5B) [46]. Synaptic
200 homeostasis is blocked in *inc* mutants and is restored by Inc expressed post-synaptically in muscle
201 with *BG57-Gal4* [20] (Fig 5A and 5B). We assessed whether Inc^{F105A}, which impairs Cul3
202 associations and rescue of sleep (Figs 2B, 3B, and 3C), could restore synaptic homeostasis to *inc*
203 mutants. In contrast to wild-type Inc, post-synaptic expression of Inc^{F105A} failed to restore synaptic
204 homeostasis to Inc mutants, indicating that Inc-Cul3 associations are required for Inc activity at
205 synapses (Fig 5B). To determine whether the activity of Cul3-Inc complexes requires the Inc C-
206 terminus, we similarly assessed the rescuing activity of Inc^{1-123}, which lacks this conserved
207 domain. Inc^{1-123} failed to restore synaptic homeostasis to *inc* mutants (Fig 5A and 5B), indicating
208 that the C-terminus of Inc is essential for Inc activity at synapses. The requirement for Inc-Cul3
209 associations and the Inc C-terminus for both normal sleep and synaptic plasticity supports the
210 notion that Inc serves as a Cul3 adaptor in vivo.
211

212 **Mutation of a conserved disease-associated arginine abolishes Inc function and defines a**
213 **surface likely to recruit substrates**

214 To further dissect Inc function, we mutated conserved C-terminal residues we hypothesized
215 might bind Inc targets (Fig 6A). In particular, a missense mutation of a conserved arginine
216 (R145H) in the human Inc ortholog KCTD17 is associated with myoclonic dystonia, a movement
217 disorder [37]. While the mechanism of KCTD17^{R145H} pathogenesis is unknown, the analogous
218 KCTD5 residue resides on the surface of the C-terminal domain (S1D Fig). We reasoned that this
219 residue might have a conserved function in binding substrates, and we therefore mutated the
220 corresponding Inc residue (Inc^{R135H}) to assess its function. We also mutated three Inc residues
221 (N167, Y168, G169) to alanine (Inc^{AAA}); the corresponding KCTD5 residues reside in an exposed
222 loop that might recruit substrates (S1D Fig).

223 In S2 cells, Inc^{R135H} and Inc^{AAA} were stable and associated with Cul3 and Inc
224 indistinguishably from wild-type Inc (Figs 6B and 6C), indicating that these mutations do not alter
225 Inc multimerization or Cul3 binding. In vivo, Inc^{R135H} and Inc^{AAA} were stably expressed with *inc-*
226 *Gal4* (Fig 6D) and lacked dominant negative activity when expressed in neurons or with *inc-Gal4*
227 (S6C–D Fig). Next, we tested whether Inc^{R135H} and Inc^{AAA} could rescue the sleep deficits of *inc*
228 mutants. When expressed with *inc-Gal4*, Inc^{AAA} rescued *inc^{1}* mutants indistinguishably from wild-
229 type Inc, indicating that Inc^{AAA} retains normal activity (Fig 6E and 6F and S8 Fig and S10A–D
230 Fig). In stark contrast, Inc^{R135H} was unable to restore sleep to *inc^{1}* mutants, indicating that the
231 R135H mutation abolishes Inc function (Fig 6E and 6F and S10A–D Fig). The complete loss of
232 Inc activity caused by the R135H mutation is indistinguishable from the consequences of deleting
233 the Inc C-terminus (Fig 4B and 4C), suggesting that R135 is essential for the function of the C-
234 terminus and binding Inc targets. These findings furthermore suggest that the analogous

235 KCTD17^{R145H} mutation causes myoclonic dystonia by impairing the recruitment and
236 ubiquitination of KCTD17 targets.
237
238 **Inc exhibits properties of a Cul3 adaptor in neurons and is negatively regulated by Cul3**
239 Normal sleep requires the activity of both *inc* and *Cul3* in neurons [17,18]. We performed
240 several experiments to determine whether Inc has the properties of a Cul3 adaptor in vivo. First,
241 we tested whether Inc-Cul3 complexes assemble in vivo, by co-expressing epitope-tagged Inc and
242 Cul3 with *inc-Gal4* and performing co-immunoprecipitations. We observed that Inc and Cul3
243 associate in vivo (Fig 7A). Second, we tested whether Inc multimerizes in vivo, by assessing the
244 physical interactions of Inc-HA and Myc-Inc co-expressed with *inc-Gal4*. These proteins
245 associated robustly (Fig 7B), indicating that Inc forms homomultimers in vivo. Third, we tested
246 whether Inc is regulated by Cul3. Cul3 adaptors are often regulated by autocatalytic ubiquitination
247 and degradation in Cul3 complexes [22,47–49]. Neuronal RNAi against *Cul3* increased Inc protein
248 levels in head lysates (Fig 7C), indicating that Cul3 negatively regulates Inc abundance. qRT-PCR
249 confirmed that neuronal Cul3 RNAi reduced Cul3 mRNA levels in heads (Fig 7D), as reported
250 previously [50], but did not significantly alter *inc* transcript levels (Fig 7D). These findings
251 indicate that Cul3 negatively regulates Inc by a post-transcriptional mechanism. We conclude that
252 Inc is likely regulated by Cul3-dependent autocatalytic ubiquitination and degradation in neurons,
253 cells through which *inc* influences sleep [17,18]. Together, these results indicate that Inc has the
254 attributes of a Cul3 adaptor in vivo.
255
256 **Discussion**
257 *Cul3* mutations disrupt brain development and physiology and contribute to neurological
258 disorders, including autism and schizophrenia. Understanding the diverse functions of *Cul3* in the

259 nervous system requires characterization of its relevant adaptors and substrates. Our findings
260 implicate Inc as a Cul3 adaptor critical for sleep and synaptic function. We have shown that Inc-
261 Cul3 complexes assemble in vivo, that weakening Inc-Cul3 associations impairs Inc activity, and
262 that Inc has modular functional domains typical of Cul3 adaptors. The conserved C-terminal
263 domain of Inc is vital for Inc activity but dispensable for Inc multimerization and Cul3 binding, as
264 expected of a substrate recruitment domain. Lastly, the negative regulation of Inc abundance by
265 Cul3 in vivo is characteristic of autocatalytic adaptor ubiquitination within the Cul3 complex and
266 subsequent proteolytic degradation.

267 In addition to demonstrating that Inc is regulated by autocatalytic ubiquitination, the
268 present findings suggest that Inc activity is controlled by additional mechanisms. Inc mutants
269 deficient for Cul3 binding would be expected to sequester substrates but do not perturb sleep when
270 overexpressed. Similarly, C-terminally truncated Inc mutants that cannot recruit substrates might
271 be expected to compete for Cul3 binding and inhibit ubiquitination of Inc substrates, yet these
272 mutants lack dominant negative activity. Consistent with these findings, overexpression of wild-
273 type Inc rescues *inc* mutants in a permissive manner but does not cause gain-of-function
274 phenotypes, for both sleep and synaptic homeostasis [17,20,33]. Inc may thus be regulated by
275 mechanisms that control its ability to bind Cul3, recruit substrates, or catalyze substrate
276 ubiquitination.

277 Inc and its orthologs are structurally distinct from better characterized Cul3 adaptors of the
278 BTB-MATH and BTB-BACK-Kelch families. In contrast to BTB-MATH and BTB-BACK-Kelch
279 adaptors that form homodimers and bind Cul3 independently [40–42], Inc orthologs form
280 homopentamers that bind Cul3 in radial assemblies [39,43,45,51–53]. Our findings indicate that
281 Cul3 binds to a cleft between adjacent Inc subunits, consistent with a similar homopentameric
282 structure for Cul3-Inc complexes. Because formation of higher order Cul3 complexes can

283 stimulate substrate ubiquitination [40], the pentameric structure of Inc and its orthologs may enable
284 efficient ubiquitination of substrates, including those that associate weakly or transiently with the
285 Cul3 complex.

286 The analysis of C-terminal Inc truncations and point mutations suggests a mechanism by
287 which Inc and its orthologs bind substrates. Deleting the 25 C-terminal residues of Inc reduces but
288 does not abolish Inc activity, indicating that these residues contribute to substrate binding. The
289 analogous KCTD5 residues are not resolved in crystal structures of KCTD alone [39] (Fig. S1D),
290 suggesting that they are flexible and may become structured upon target binding. Second, mutation
291 of a surface-exposed arginine (R135) abolishes Inc function and is functionally equivalent to
292 deleting the C-terminus. Together, these data support a model in which R135 and the surrounding
293 lateral surface of Inc bind substrates in conjunction with the C-terminal tail of Inc. A recent
294 structure of KCTD5 bound to a substrate provides direct support for this mechanism [53].
295 Furthermore, this mechanism may be conserved in other Inc orthologs and disrupted by
296 KCT17^{R145H} mutations linked to myoclonic dystonia [37]. While the simplest hypothesis is that
297 Inc binds substrates directly, Inc might also engage co-adaptor proteins, analogous to the
298 mechanism described for the BTB-Kelch adaptor KLHL12 [54].

299 Our findings do not identify Inc targets that mediate its impact on sleep and synaptic
300 homeostasis in *Drosophila*, nor do they discern whether Inc orthologs contribute to changes in
301 sleep or other *Cul3* phenotypes in mammals. Another important unresolved question is whether
302 heterozygous loss-of-function *Cul3* mutations alter sleep in rodent models, analogous to sleep
303 disturbances reported for human *Cul3* mutations associated with autism [4]. While Inc orthologs
304 are expressed in the mammalian brain [33], their characterization in vivo remains limited. In mice,
305 *KCTD5* deletions are homozygous lethal and cause motor deficits when heterozygous [55];
306 possible effects on sleep have not yet been assessed. There are no existing rodent models for

307 mutations in *KCTD2* or *KCTD17*. Conditional genetic analysis of *inc* in flies and *Cul3* in mice
308 underscores developmental mechanisms of action. Inc acts in developing neurons to impact sleep
309 in adult flies [56], suggesting that its relevant substrates have developmental functions within the
310 brain. Conditional deletion of *Cul3* in mice indicates that its behavioral phenotypes, including
311 deficits in sociability and cognition, arise during a critical period of brain development [10],
312 suggesting that any sleep phenotypes of *Cul3* mutants might also arise in a developmental manner.

313 The molecular targets of Inc that influence sleep are likely conserved, as mammalian Inc
314 orthologs restore sleep to *inc* mutants [33]. Intriguing overlaps in the synaptic phenotypes of *inc*
315 and *Cul3* mutants in flies and mice suggest that Inc orthologs impact synaptic function through
316 substrates that are similarly conserved. Inc and Cul3 are required in flies for synaptic homeostasis
317 at glutamatergic neuromuscular synapses and are recruited to synapses during homeostatic
318 potentiation [20]. *Cul3* mutations in mice alter glutamatergic neurotransmission and the abundance
319 of glutamate receptors and other synaptic proteins [9,11]. While contributions of mammalian Inc
320 orthologs to *Cul3* phenotypes at glutamatergic synapses remain unexplored, Cul3 and Inc
321 orthologs are present in synaptosome preparations [33], suggesting that their targets include
322 synaptic proteins.

323 Characterization of Inc orthologs has identified various substrates in cultured cells. c-Myc
324 is a substrate for KCTD2 [57], and KCTD5 ubiquitinates ΔNp63α and RhoGDI [58,59], linking
325 KCTD2 and KCTD5 to pathways that regulate cell proliferation. KCTD5 has also been shown to
326 ubiquitinate a G-protein beta subunit and to regulate AKT and cAMP signaling, including in
327 cultured striatal neurons [55,60,61]. KCTD17 ubiquitinates trichoplein, a regulator of primary cilia
328 [62], as well as Chop and PHLPP2 [63,64], proteins that regulate lipids and adipogenesis. Whether
329 these targets or others mediate the impact of Inc on sleep and synapses remains unknown.

330 Emerging evidence from genetic studies in humans suggests that Inc orthologs have
331 functions in the brain that remain poorly understood. As noted above, *KCTD17* mutations are
332 associated with myoclonic dystonia [37]. Polymorphisms near the *KCTD2* locus are associated
333 with Alzheimer's [65], and another study suggests an association of *KCTD5* and daytime
334 sleepiness [66]. Elucidating targets of Cul3-Inc complexes within the fly brain may provide a
335 powerful system to understand conserved mechanisms through which Cul3 and Inc contribute to
336 nervous system function and neurological disorders.

Acknowledgements

We thank J. Lopez for assistance with Western blots and qRT-PCR; Z. Zuchowski for assistance in constructing plasmids; A. Arzeno and A. Gonzalez for assistance with immunoprecipitations; and N. Ringstad, J. Treisman, and members of the Stavropoulos laboratory for comments on the manuscript. This work was supported by an International Student Research Fellowship from the Howard Hughes Medical Institute (HHMI) to Q.L., by a grant from the National Institutes of Health (NS091546) to D.D., and by grants from the National Institutes of Health (NS112844 and NS111304), the Mathers Foundation, Whitehall Foundation grant 2013-05-78, fellowships from the Alfred P. Sloan and Leon Levy Foundations, a NARSAD Young Investigator Award from the Brain and Behavior Foundation, the J. Christian Gillin, M.D. Research Award from the Sleep Research Society Foundation, and a Career Scientist Award from the Irma T. Hirschl/Weill-Caulier Trust to N.S.

Author Contributions

Conceptualization: Q.L., D.D., N.S.

Investigation: Q.L., K.Y.L., R.A., F.V., C.D., J.M., X.L., and N.S.

Resources: Q.L., D.D., and N.S.

Writing - original draft: N.S. and Q.L.

Writing - review and editing: N.S., Q.L., and D.D.

Competing Interests

The authors declare that no completing interests exist.

361 **Materials and methods**

362 **Plasmids and molecular cloning**

363 Vectors for expression in S2 cells were as follows:

364 pAc5.1–Inc-HA (pNS277) encodes Inc fused to a C-terminal HA epitope
365 (GSYPYDVPDYA) and was generated by ligating EcoRI-XhoI digested pAc5.1/V5-HisA
366 backbone (ThermoFisher) and an EcoRI-XhoI Inc-HA fragment from pNS273 (described below).

367 pAc5.1–3×Myc-Inc (pNS351) was previously described (Li et al., 2017) and encodes an
368 N-terminal 3×Myc epitope (MEQKLISEEDLGSEQKLISEEDLGSEQKLISEEDLAS) fused to
369 Inc.

370 pAc5.1–3×Myc-Inc$^{22-211}$ (pNS370) was generated by ligating NheI-XhoI digested pNS309
371 (Stavropoulos and Young, 2011) and the NheI-XhoI fragment liberated from the PCR
372 amplification product of pNS351 template and primers oNS315 and oNS285.

373 pAc5.1–3×Myc-Inc$^{31-211}$ (pNS371) was generated similarly to pNS370, substituting
374 primers oNS316 and oNS285.

375 pAc5.1–3×Myc-Inc$^{124-211}$ (pNS372) was generated similarly to pNS370, substituting
376 primers oNS317 and oNS285.

377 pAc5.1–3×Myc-Inc$^{1-123}$ (pNS374) was generated similarly to pNS370, substituting primers
378 oNS277 and oNS319.

379 pAc5.1–3×Myc-Inc$^{1-156}$ (pNS375) was generated similarly to pNS370, substituting primers
380 oNS277 and oNS320.

381 pAc5.1–3×Myc-Inc$^{1-186}$ (pNS376) was generated similarly to pNS370, substituting primers
382 oNS277 and oNS321.

383 pAc5.1–3×Myc-Inc$^{22-123}$ (pNS377) was generated similarly to pNS370, substituting
384 primers oNS315 and oNS319.

385 pAc5.1–3×HA-Inc (pNS402) encodes an N-terminal 3×HA epitope
386 (MYPYDVPDYAGSYPYDVPDYAGSYPYDVPDYAAS) fused to Inc and was generated by
387 ligating NheI-XhoI digested pNS310 (Stavropoulos and Young, 2011) and an NheI-XhoI *inc*
388 fragment liberated from pNS351.

389 pAc5.1–3×FLAG-Cul3 (pNS403) encodes an N-terminal 3×FLAG epitope
390 (MDYKDDDDKGSDYKDDDDKGSDYKDDDDKAS) fused to *Drosophila* Cul3 and was
391 generated by ligating NheI-NotI digested pNS311 and an NheI-NotI Cul3 fragment liberated from
392 pNS314 (Stavropoulos and Young, 2011). pNS311 contains an N-terminal 3×FLAG tag and was
393 generated from pNS298, a pAc5.1/V5-HisA derivative that contains a C-terminal 3×FLAG tag.
394 To construct pNS298, oligonucleotides oNS234 and oNS235 were phosphorylated, annealed, and
395 cloned into XhoI-XbaI digested pAc5.1/V5-HisA. To construct pNS311, EcoRI-NotI digested
396 pAc5.1/V5-HisA was ligated to the EcoRI-NotI fragment liberated from the PCR amplification
397 product of pNS298 template and primers oNS240 and oNS241.

398 pAc5.1–3×FLAG-Inc (pNS408) encodes an N-terminal 3×FLAG epitope
399 (MDYKDDDDKGSDYKDDDDKGSDYKDDDDKAS) fused to Inc and was generated by
400 ligating NheI-NotI digested pNS311 and an NheI-XhoI *inc* fragment liberated from pNS351.

401 pAc5.1–3×HA-Inc^{F47A} (pNS409) encodes an N-terminal 3×HA epitope
402 (MYPYDVPDYAGSYPYDVPDYAGSYPYDVPDYAAS) fused to Inc^{F47A} and was generated by
403 ligating NheI-XhoI digested pNS310 and an NheI-XhoI digested Inc^{F47A} fragment. The Inc^{F47A}
404 fragment was prepared by fusion PCR in two steps. First, overlapping 5' and 3' Inc^{F47A} fragments
405 were generated by PCR amplification of pNS408 template with primers oNS277/oNS695 and
406 oNS684/oNS694, respectively. An equimolar mix of these fragments was then used as template
407 for fusion PCR amplification with primers oNS277 and oNS684.

408 pAc5.1–3×HA-Inc^{R50E} (pNS410) was generated similarly to pNS409, substituting primers
409 oNS277/oNS697 and oNS684/oNS696 to obtain 5' and 3' Inc^{R50E} fragments, respectively.
410 pAc5.1–3×HA-Inc^{D57A} (pNS411) was generated similarly to pNS409, substituting primers
411 oNS277/oNS699 and oNS684/oNS698 to obtain 5' and 3' Inc^{D57A} fragments, respectively.
412 pAc5.1–3×HA-Inc^{D61A} (pNS412) was generated similarly to pNS409, substituting primers
413 oNS277/oNS701 and oNS684/oNS700 to obtain 5' and 3' Inc^{D61A} fragments, respectively.
414 pAc5.1–3×HA-Inc^{E104K} (pNS413) was generated similarly to pNS409, substituting primers
415 oNS277/oNS703 and oNS684/oNS702 to obtain 5' and 3' Inc^{E104K} fragments, respectively.
416 pAc5.1–3×HA-Inc^{F105A} (pNS419) was generated similarly to pNS409, substituting primers
417 oNS277/oNS1123 and oNS684/oNS1122 to obtain 5' and 3' Inc^{F105A} fragments, respectively.
418 pAc5.1–3×HA-Inc^{Y106F} (pNS420) was generated similarly to pNS409, substituting primers
419 oNS277/oNS1146 and oNS684/oNS1145 to obtain 5' and 3' Inc^{Y106F} fragments, respectively.
420 pAc5.1–3×HA-Inc^{N107A} (pNS421) was generated similarly to pNS409, substituting primers
421 oNS277/oNS1125 and oNS684/oNS1124 to obtain 5' and 3' Inc^{N107A} fragments, respectively.
422 pAc5.1–3×FLAG-Inc^{D73A} (pNS430) and pAc5.1–3×FLAG-Inc^{N82A} (pNS431) were
423 generated simultaneously, using PCR amplification of pNS408 template with primers
424 oNS277/oNS686 and oNS684/oNS685 to generate overlapping Inc^{N82A} and Inc^{D73A} fragments,
425 respectively. An equimolar mix of these fragments was used as template for fusion PCR
426 amplification with primers oNS277 and oNS684, and the PCR product was digested with NheI-
427 XhoI and ligated to NheI-XhoI digested pNS311. Sequencing of multiple clones identified both
428 single mutants.
429 pAc5.1–3×FLAG-Inc^{K88D} (pNS432) and pAc5.1–3×FLAG-Inc^{E101K} (pNS433) were
430 generated similarly to pNS430 and pNS431, substituting primers oNS277/oNS688 and
431 oNS684/oNS687 to obtain overlapping Inc^{E101K} and Inc^{K88D} fragments, respectively.

432 pAc5.1–3×FLAG-Inc^{T36A} (pNS434) and pAc5.1–3×FLAG-Inc^{D71A} (pNS435) were
433 generated similarly to pNS430 and pNS431, substituting primers oNS277/oNS693 and
434 oNS684/oNS689 to obtain overlapping Inc^{D71A} and Inc^{T36A} fragments, respectively.
435 pAc5.1–3×HA-Inc^{R85E} (pNS436) was generated similarly to pNS430 and pNS431,
436 substituting primers oNS277/oNS692 and oNS684/oNS691 to obtain overlapping Inc^{R85E} and
437 Inc^{D71A} fragments, respectively, and NheI-XhoI digested pNS310. Inc^{R85E} was identified by
438 sequencing multiple clones.
439 pAc5.1–3×HA-Inc$^{F47A/F105A}$ (pNS422) was generated similarly to pNS409, substituting
440 pNS409 as template and primers oNS277/oNS1123 and oNS684/oNS1122 to obtain 5' and 3'
441 Inc$^{F47A/F105A}$ fragments, respectively.
442 pAc5.1–3×HA-Inc$^{D73A/N82A}$ (pNS414) was generated similarly to pNS409, substituting
443 pNS430 template and primers oNS277/oNS686 to obtain the 5' Inc$^{D73A/N82A}$ fragment and pNS431
444 template and primers oNS684/oNS685 to obtain the 3' Inc$^{D73A/N82A}$ fragment.
445 pAc5.1–3×HA-Inc$^{K88D/E101K}$ (pNS415) was generated similarly to pNS409, substituting
446 pNS432 template and primers oNS277/oNS688 to obtain the 5' Inc$^{K88D/E101K}$ fragment and pNS433
447 template and primers oNS684/oNS687 to obtain the 3' Inc$^{K88D/E101K}$ fragment.
448 pAc5.1–3×HA-Inc$^{T36A/D71A}$ (pNS416) was generated similarly to pNS409, substituting
449 pNS434 template and primers oNS277/oNS693 to obtain the 5' Inc$^{T36A/D71A}$ fragment and pNS435
450 template and primers oNS684/oNS689 to obtain the 3' Inc$^{T36A/D71A}$ fragment.
451 pAc5.1–3×HA-Inc$^{D71A/R85E}$ (pNS417) was generated similarly to pNS409, substituting
452 pNS435 template and primers oNS277/oNS692 to obtain the 5' Inc$^{D71A/R85E}$ fragment and pNS436
453 template and primers oNS684/oNS691 to obtain the 3' Inc $^{D71A/R85E}$ fragment.

454 pAc5.1–3×HA-Inc$^{T36A/D71A/R85E}$ (pNS418) was generated by ligating EcoRV-XhoI
455 digested pNS434 backbone and an Inc$^{D71A/R85E}$ fragment obtained by EcoRV-XhoI digestion of
456 the PCR amplification product of pNS417 template and primers oNS277 and oNS684.
457 pAc5.1–3×HA-Inc^{R135H} (pNS426) was generated by ligating HindIII-XhoI digested
458 pNS402 backbone and a HindIII-XhoI Inc^{R135H} fragment. The Inc^{R135H} fragment was prepared by
459 fusion PCR in two steps. First, overlapping 5' and 3' Inc^{R135H} fragments were generated by PCR
460 amplification of pNS346 template with primers oNS1126/oNS1555 and oNS1127/oNS1554,
461 respectively. An equimolar mix of these fragments was then used as template for fusion PCR
462 amplification with primers oNS1126 and oNS1127. pUASTattB–Myc-Inc (pNS346) encodes an
463 N-terminal Myc epitope (MEQKLISEEDLAS) fused to Inc, as previously described (Li et al.,
464 2017).
465 pAc5.1–3×HA-Inc^{AAA} (pNS427) was generated similarly to pNS426, substituting a
466 HindIII-XhoI Inc^{AAA} fragment generated similarly with fusion PCR; primer pairs
467 oNS1126/oNS1557 and oNS1127/oNS1556 were used to obtain 5' and 3' Inc^{AAA} fragments,
468 respectively.
469 pAc5.1–3×Myc-Inc$^{T36A/D71A/R85E}$ (pNS437) was generated by ligating NheI-XhoI digested
470 pNS309 backbone and an NheI-XhoI Inc$^{T36A/D71A/R85E}$ fragment liberated from pNS418.
471 pAc5.1–3×Myc-Inc^{F47A} (pNS438) was generated by ligating NheI-XhoI digested pNS309
472 backbone and an NheI-XhoI Inc^{F47A} fragment liberated from pNS409.
473 pAc5.1–3×Myc-Inc^{F105A} (pNS439) was generated by ligating NheI-XhoI digested pNS309
474 backbone and an NheI-XhoI Inc^{F105A} fragment liberated from p419.
475 pAc5.1–3×Myc-Inc$^{F47A/F105A}$ (pNS440) was generated by ligating NheI-XhoI digested
476 pNS309 backbone and an NheI-XhoI Inc$^{F47A/F105A}$ fragment liberated from pNS422.

477 pAc5.1–3×Myc-Inc^{R135H} (pNS441) was generated by ligating HindIII-XhoI digested
478 pNS351 backbone and a HindIII-XhoI Inc^{R135H} fragment prepared as for pNS426.
479 pAc5.1–3×Myc-Inc^{AAA} (pNS442) was generated by ligating HindIII-XhoI digested
480 pNS351 backbone and a HindIII-XhoI Inc^{AAA} fragment prepared as for pNS427.
481
482 Vectors for *Drosophila* transgenesis were as follows:
483 pUASTattB–Myc-Inc^{R135H} (pNS428) was generated by ligating a BglII-XhoI digested
484 pUASTattB backbone (Bischof et al., 2007), prepared by liberating an unrelated BglII-XhoI insert,
485 and a BgII-XhoI digested Myc-Inc^{R135H} fragment, generated with fusion PCR as for pNS426.
486 pUASTattB–Myc-Inc^{AAA} (pNS429) was generated by ligating a BgII-XhoI pUASTattB
487 backbone prepared from pNS349 [33] and a BgII-XhoI digested Myc-Inc^{AAA} fragment, generated
488 with fusion PCR as for pNS427.
489 pUAST–Inc-HA (pNS273) was previously described and encodes Inc fused to a C-terminal
490 HA epitope (GSYPYDVPDYA) [33].
491 pUASTattB–3×FLAG-Inc (pNS404) encodes an N-terminal 3×FLAG epitope
492 (MDYKDDDDKGSDYKDDDDKGSDYKDDDDKAS) fused to Inc and was generated by three-
493 piece ligation of EcoRI-XhoI digested pUASTattB, an EcoRI-NheI 3×FLAG fragment liberated
494 from the PCR amplification product of pNS311 template and primers ACF and oNS241, and an
495 NheI-XhoI *inc* fragment liberated from pNS351.
496 pUASTattB–3×FLAG-Inc$^{1-186}$ (pNS405) was generated similarly to pNS404, substituting
497 an NheI-XhoI Inc$^{1-186}$ fragment liberated from pNS376.
498 pUASTattB–3×FLAG-Inc$^{1-156}$ (pNS406) was generated similarly to pNS404, substituting
499 an NheI-XhoI Inc$^{1-156}$ fragment liberated from pNS375.

500 pUASTattB–3×FLAG-Inc$^{1-123}$ (pNS407) was generated similarly to pNS404, substituting
501 an NheI-XhoI Inc$^{1-123}$ fragment liberated from pNS374.
502 pUASTattB–3×FLAG-Inc^{F47A} (pNS423) was generated similarly to pNS404, substituting
503 an NheI-XhoI Inc^{F47A} fragment liberated from pNS409.
504 pUASTattB–3×FLAG-Inc^{F105A} (pNS424) was generated similarly to pNS404, substituting
505 an NheI-XhoI Inc^{F105A} fragment liberated from pNS419.
506 pUASTattB–3×FLAG-Inc$^{F47A/F105A}$ (pNS425) was generated similarly to pNS404,
507 substituting an NheI-XhoI Inc$^{F47A/F105A}$ fragment liberated from pNS422.
508
509 **Oligonucleotides**
510 Oligonucleotides used in this work, listed 5' to 3', are as follows:
511 oNS180 ACGTAGATCTGAACCGCAGCAGCGGCAACACCATC
512 oNS184 CCAGCCATCCGACAGCGTTGAGATC
513 oNS234
514 TCGAGGCTAGCGACTACAAGGATGATGACGATAAGGGCTCCGATTACAAGGA
515 CGACGATGATAAGGGATCCGATTACAAGGATGATGACGACAAGTGAT
516 oNS235
517 CTAGATCACTTGTCGTCATCATCCTTGTAATCGGATCCCTTATCATCGTCGTCC
518 TTGTAATCGGAGCCCTTATCGTCATCATCCTTGTAGTCGCTAGCC
519 oNS240
520 ACTGGAATTCCGCGGCAACATGGACTACAAGGATGATGACGATAAGGGC
521 oNS241
522 ACTGGCGGCCGCTCCTAGGGTGCTAGCCTTGTCGTCATCATCCTTGTAATCGG
523 AT

524	oNS277	ACGTGCTAGCATGAGCACGGTGTTCATAAACTCGC
525	oNS285	ACGTGCTAGCTCGAGGGGTTGTGTGTGAATATATAGCGCGA
526	oNS315	ACGTGCTAGCCAGTGGGTCAAGCTGAACGTAG
527	oNS316	ACGTGCTAGCACCTACTTCCTCACCACAAAGACG
528	oNS317	ACGTGCTAGCCAGCGACCCCAAACGGACAA
529	oNS319	ACGTCTCGAGTTAATCCCTGTGCAGGATGCACTC
530	oNS320	ACGTCTCGAGTTACCTCCAGCCATCCGACAG
531	oNS321	ACGTCTCGAGTTATGTGCCACACTCTTTGGATACCA
532	oNS337	TTTTTTTTTTTTTTTTTTTTTTTVN
533	oNS684	ACGTCTCGAGGGGTTGTGTGTGAATATATAGCGCGA
534	oNS685	CCTGATCGACAGAGCCCCCAAATACTTTGC
535	oNS686	GGCGCAGGTAGGCGAGCACGGGTGCAAA
536	oNS687	TGCGCCACGGCGACCTTGTGCTCGAT
537	oNS688	TAGAACTCAGCCTCCTTCAGGACGCCTTC
538	oNS689	CTACTTCCTCACCGCCAAGACGACGCTC
539	oNS691	GCCTACCTGATCGCCAGAGACCCCAAA
540	oNS692	CAAGCTTGCCGTGTTCCAGGTAATTGAGC
541	oNS693	TTTGGGGTCTCTGGCGATCAGGTAGGC
542	oNS694	GACCCAAATTCGGCCCTCTCCCGTCTG
543	oNS695	CAGACGGGAGAGGGCCGAATTTGGGTC
544	oNS696	TCGTTCCTCTCCGAACTGATTCAGGAGG
545	oNS697	CCTCCTGAATCAGTTCGGAGAGGAACGA
546	oNS698	CAGGAGGACTGCGCCTTGATATCAGATCG
547	oNS699	CGATCTGATATCAAGGCGCAGTCCTCCTG

548 oNS700 CGACTTGATATCAGCCCGGGACGAGAC

549 oNS701 GTCTCGTCCCGGGCTGATATCAAGTCG

550 oNS702 CCTGGAGGAGGCTAAGTTCTACAACGTGAC

551 oNS703 GTCACGTTGTAGAACTTAGCCTCCTCCAGG

552 oNS1122 GGAGGCTGAGGCCTACAACGTGAC

553 oNS1123 GTCACGTTGTAGGCCTCAGCCTCC

554 oNS1124 GCTGAGTTCTACGCCGTGACGCAGC

555 oNS1125 GCTGCGTCACGGCGTAGAACTCAGC

556 oNS1126 CAACTGCAACTACTGAAATCTGCCAAGAAG

557 oNS1127 GGTAGTTTGTCCAATTATGTCACACCACAGAAG

558 oNS1145 GAGGCTGAGTTCTTCAACGTGACGCAGC

559 oNS1146 GCTGCGTCACGTTGAAGAACTCAGCCTC

560 oNS1554 AAGCGCGTTTATCATGTGCTGCAGTGC

561 oNS1555 GCACTGCAGCACATGATAAACGCGCTT

562 oNS1556

563 ATCAGCATGCAGTACACGGCCGCCGCGCCCTTCGAAAACAATGAGTTCCTG

564 oNS1557 ATTGTTTTCGAAGGGCGCGGCGGCCGTGTACTGCATGCTGATCAGCT

565 oNS1783 TGTCCACGTACCAGATGTGTGTGCTA

566 oNS1784 ACTAGCAAGTTGTGAGCCAGACGC

567 ACF GACACAAAGCCGCTCCATCAG

568 RPS3A CGAACCTTCCGATTTCCAAGAAACGC

569 RPS3B ACGACGGACGGCCAGTCCTCC

570

571 **Cell culture and biochemistry**

572 S2 cells were cultured in S2 media containing 10% FBS, penicillin, and streptomycin, and
573 were transfected with Effectene (Qiagen) as described previously (Stavropoulos and Young,
574 2011). Transfections were performed in 6 well plates for ~24 hr, after which liposome-containing
575 media was replaced with fresh culture media. 400 ng of total DNA was used for each transfection.
576 For transfections involving two plasmids, an equal amount of each was used. For comparisons of
577 multiple plasmids, empty vector lacking insert was used to equalize DNA amounts as required.
578 Cells were harvested 36-48 hr after transfection, washed in PBS, and lysed in ice-cold NP40 lysis
579 buffer (50 mM Tris pH 7.6, 150mM NaCl, 0.5% NP40) containing protease inhibitors (Sigma,
580 P8340). Protein extracts were quantitated in duplicate (BioRad, 5000111). For measurements of
581 protein stability, 100 µg/ml cycloheximide (Fisher, AC357420010) was added at specified
582 timepoints prior to lysis.

583 For immunoprecipitations of truncated Inc proteins and Inc point mutants from S2 cells,
584 300-1000 µg of total protein was incubated overnight at 4°C with 1:100 anti-FLAG (Sigma,
585 F1804), anti-Myc (Sigma, C3956), or rat anti-Inc antibody [17], followed by incubation with 20
586 µl (50% slurry) of protein G sepharose beads (ThermoFisher, 10-1243) at 4°C on a nutator for 1
587 hr or overnight. Alternatively, 20 µl (50% slurry) of anti-FLAG (Sigma, F2426) or anti-Myc
588 affinity gel (Sigma, E6654) was used to immunoprecipitate samples. Samples were washed 4×5
589 min at 4°C with NP40 lysis buffer, denatured in SDS sample buffer, separated on Tris SDS-PAGE
590 gels, and transferred to nitrocellulose.

591 Protein extracts were prepared from whole flies or sieved heads by manual pestle
592 homogenization in ice-cold NP40 lysis buffer containing protease inhibitors. To assess in vivo
593 expression of Inc proteins, 30 µg of lysate was separated on Tris-SDS-PAGE gels. For
594 immunoprecipitations of whole fly extracts, 800 µg of protein was incubated with 30 µl (50%

595 slurry) of anti-Myc affinity gel for 1.5 hr at 4°C on a nutator. Samples were washed, denatured,
596 electrophoresed, and transferred to membranes as described above.
597
598 **Western blots and antibodies**
599 Membranes were incubated for 60-90 min at room temperature in blocking buffer (LI-
600 COR, 927-40000). Membranes were subsequently incubated for 1-2 hr at room temperature or 4°C
601 overnight in blocking buffer containing 0.1% Tween 20 and the appropriate primary antibodies:
602 rabbit anti-Myc (1:2,000, Sigma, C3956), mouse anti-FLAG (1:2,000, Sigma, F1804), rat anti-HA
603 (1:2,000, Roche, 11867431001), and rabbit anti-HA (1:2,000, Bethyl Laboratories, A190-208A),
604 mouse anti-tubulin (1:10,000, DSHB, 12G10), and rabbit anti-tubulin (1:60,000, VWR, 89364-
605 004). Membranes were washed 4×5 min in TBST (150 mM NaCl, 10mM Tris pH 7.6, and 0.1%
606 Tween 20) and subsequently incubated in the dark for 30-60 min at room temperature in blocking
607 buffer containing 0.1% Tween 20, 0.01% SDS, and appropriate secondary antibodies, all diluted
608 1:15,000 or 1:30,000: Alexa 680 donkey anti-rabbit (Life Technologies, A10043), Alexa 790 anti-
609 rabbit (Life Technologies, A11374), Alexa 680 donkey anti-mouse (Life Technologies, A10038),
610 Alexa 790 anti-mouse (Life Technologies, A11371), Alexa 790 anti-rat (Jackson
611 ImmunoResearch, 712-655-153), and Alexa 680 donkey anti-rat (Jackson ImmunoResearch, 712-
612 625-1533). Membranes were then washed 4×5 min in TBST, 1×5 min in TBS, and imaged on a
613 Li-Cor Odyssey CLx instrument.
614
615 **qRT-PCR**
616 Total RNA was isolated from adult male fly heads with TRIZOL (ThermoFisher, 15596-
617 026). 5 µg of RNA was reverse transcribed with $d(T)_{23}VN$ primer (oNS337) and SuperScript II
618 reverse transcriptase (ThermoFisher, 18064014). qPCR was performed using a BioRad DNA

619 Engine Opticon 2 System, SYBR Green Supermix (Bio-Rad, 1725272), and the following primers:
620 oNS180 and oNS184 (*inc*); oNS1783 and oNS1784 (*Cul3*); RPS3A and RPS3B (*rps3*).
621
622 **Fly stocks and transgenes**
623 *elav*^{c155}*-Gal4* [67], *inc*^{1} [17], *inc*^{kk3} [20], *inc-Gal4* [17], *inc*^{1} *inc-Gal4* [33], *BG57-Gal4*
624 [68], *attP2: UAS-Myc-Inc* [33], *attP2: UAS-3×FLAG-Inc* [33], and *UAS-3×FLAG-3×HA-Cul3*
625 [69] were previously described. *UAS-Cul3-RNAi* (11861R-2) and *UAS-inc-RNAi* (18225) were
626 obtained from the NIG-Fly and VDRC stock centers, respectively. Transgenic flies generated in
627 this study using pUASTattB-based vectors were integrated at *attP2* [70] with phiC31 recombinase
628 (BestGene). All transgenes were backcrossed six to eight generations to Bloomington stock 5905,
629 an isogenic *w*^{1118} stock described elsewhere as iso31 [71].
630
631 **Sleep analysis**
632 Crosses were set with five virgin females and three males on cornmeal, agar, and molasses
633 food. One- to four-day old male flies eclosing from LD-entrained cultures raised at 25°C were
634 loaded in glass tubes containing cornmeal, agar, and molasses food. Animals were monitored for
635 5-7 days at 25°C in LD cycles using DAM2 monitors (Trikinetics). The first 36-48 hours of data
636 were discarded and an integral number of days of data (3-5) were analyzed using custom Matlab
637 code. Locomotor data were collected in 1 min bins. Sleep was defined by locomotor inactivity for
638 5 min or more; all minutes within inactive periods exceeding 5 min were assigned as sleep. Dead
639 animals were excluded from analysis by a combination of automated filtering and visual inspection
640 of locomotor traces. Two to four independent biological replicates were performed for all sleep
641 assays.
642

643 **Electrophysiology**

644 Two-electrode voltage clamp (TEVC) recordings were performed in muscle 6 in
645 abdominal segments 2 and 3, as previously described [20]. Muscles were clamped at −70 mV, with
646 a leak current below 5 nA. mEPSCs were recorded for 1 min from each muscle cell in the absence
647 of stimulation. Twenty EPSCs were acquired for each cell under stimulation at 0.5 Hz, using 0.5
648 ms stimulus duration and with stimulus intensity adjusted with an ISO-Flex Stimulus Isolator
649 (A.M.P.I.). To acutely block postsynaptic receptors, larvae were incubated with philanthotoxin-
650 433 (PhTx; 20 μM; Sigma) in HL-3 for 10 min. Data were analyzed using Clampfit 10.7
651 (Molecular Devices), MiniAnalysis (Synaptosoft), Excel (Microsoft), and GraphPad Prism
652 (GraphPad Software).

653

654 **Statistics**

655 Normality of data and equal variance were assessed with Shapiro-Wilk and Brown-
656 Forsythe tests, respectively. Kruskal-Wallis and Dunn's post-hoc tests were used for comparisons
657 of total sleep, daytime sleep, nighttime sleep, sleep bout length, sleep bout number, and
658 electrophysiological parameters. For other data, one-way ANOVA and Tukey post-hoc tests were
659 used for data that met the assumption of normality and equal variance; for normally distributed
660 data with unequal variance, Welch's ANOVA and Dunnet's post-hoc tests were used. Otherwise,
661 Kruskal-Wallis and Dunn's post-hoc tests were used.

662

663 **Sequence alignments**

664 Alignments were performed with Clustal Omega 2.1 and BOXSHADE. GenBank
665 accession numbers for proteins in Figure S1A are: Inc, NP_001284787; KCTD2, NP_056168;
666 KCTD5, NP_061865; KCTD17.4, NP_001269615.

667 **Figure Legends**

668

669 **Fig 1. The Inc BTB domain mediates Inc-Cul3 and Inc-Inc interactions**

670 **(A)** Schematic of N- and C-terminally truncated Inc proteins. Residues comprising the conserved
671 BTB domain (22 to 123) and C-terminal domain (CTD) (131 to 211) are indicated. **(B and C)** Co-
672 immunoprecipitation of 3×Myc-tagged Inc or Inc truncation mutants with 3×FLAG-Cul3 **(B)** or
673 Inc-HA **(C)** from transiently transfected S2 cells. LC, immunoglobulin light chain.

674

675 **Fig 2. Identification of Inc point mutants that impair Inc-Cul3 interactions**

676 **(A)** Schematic of Inc point mutants within the BTB domain. **(B-C)** Co-immunoprecipitation of
677 3×Myc-tagged Inc or Inc point mutants with 3×FLAG-Cul3 **(B)** or 3×FLAG-Inc **(C)** from
678 transiently transfected S2 cells.

679

680 **Fig 3. Inc-Cul3 binding is required for Inc activity in vivo**

681 In vivo analysis of *inc*^{1} *inc-Gal4* animals expressing 3×FLAG-tagged Inc or Inc point mutants.
682 **(A)** Immunoblot of male whole animal lysates. **(B)** Total sleep duration. Mean ± SEM is shown. n
683 = 16-58; Kruskal-Wallis, $p<0.0001$ and Dunn's tests; *$p < 0.05$; ****$p < 0.0001$; ns, not significant
684 ($p > 0.5$). **(C)** Average daily sleep traces of indicated genotypes from **(B)**. Shading represents SEM.
685 For all panels, animals are heterozygous for UAS transgenes.

686

687 **Fig 4. The conserved Inc C-terminus is required for Inc activity in vivo**

688 In vivo analysis of *inc*^{1} *inc-Gal4* animals expressing 3×FLAG-tagged Inc or Inc truncation
689 mutants. **(A)** Immunoblot of male whole animal lysates. **(B)** Total sleep duration. Mean ± SEM is
690 shown. n = 27-30; Kruskal-Wallis, $p < 0.0001$ and Dunn's tests; *$p < 0.05$; ****$p < 0.0001$; ns,

691 not significant ($p > 0.5$). **(C)** Average daily sleep traces of indicated genotypes from **(B)**. Shading
692 represents SEM. For all panels, animals are heterozygous for UAS transgenes.
693
694 **Fig 5. Inc-Cul3 associations and the Inc C-terminus are essential for synaptic homeostasis**
695 **(A)** Spontaneous and evoked electrophysiological traces at the larval NMJ in the presence and
696 absence of philanthotoxin. **(B)** Summary data for electrophysiological recordings in the presence
697 of philanthotoxin normalized to baseline values (absence of PhTx application). Homeostatic
698 plasticity is not expressed in animals bearing Inc^{F105A} or Inc^{1-123}. Mean ± SEM is shown. n = 8-27;
699 Kruskal-Wallis, $p<0.0001$ and Dunn's tests; ***$p < 0.001$; ****$p < 0.0001$; ns, not significant (p
700 > 0.5).
701
702 **Fig 6. A conserved Inc C-terminal arginine is vital for Inc activity**
703 **(A)** Schematic of Inc C-terminal point mutants. **(B and C)** Co-immunoprecipitation of 3×Myc-
704 tagged Inc or Inc point mutants with 3×FLAG-Cul3 **(B)** or 3×FLAG-Inc **(C)** from transiently
705 transfected S2 cells. **(D)** Immunoblot of lysates prepared from whole male animals expressing
706 3×Myc-tagged Inc proteins. **(E)** Total sleep duration. Mean ± SEM is shown. n = 24-45; Kruskal-
707 Wallis, $p < 0.0001$ and Dunn's tests; ns, not significant ($p > 0.05$). **(F)** Average daily sleep traces
708 of indicated genotypes from **(E)**. Shading represents SEM. For panels **(D-F)**, animals are
709 heterozygous for UAS transgenes.
710
711 **Fig 7. Inc exhibits key properties of a Cul3 adaptor in neurons in vivo**
712 **(A)** Co-immunoprecipitation of 3×FLAG-Inc and 3×FLAG-3×HA-Cul3 from male whole animal
713 lysates. Note immunoprecipitation (IP) was performed with anti-Inc antibody. **(B)** Co-
714 immunoprecipitation of Myc-Inc and Inc-HA from male whole animal lysates. **(C)** Immunoblots

715 of male head lysates. **(D)** qRT-PCR of *Cul3* and *inc* mRNA isolated from male heads. Neuronal
716 *Cul3* RNAi decreases *Cul3* transcript levels but does not significantly alter those of *inc*. Each point
717 represents an independent biological sample measured in technical triplicate. n=3-7. Mean ± SEM
718 is shown. For *Cul3*, one-way ANOVA, $p < 0.05$ and Tukey tests; for *inc*, Kruskal-Wallis; *$p <$
719 0.05; ns, not significant ($p > 0.25$).

720 **Supporting Information**

721 **S1 Fig. Mutagenesis of Inc**

722 **(A)** Alignment of Inc and its human orthologs. Identical and similar residues are shaded in black
723 and gray respectively. Locations of Inc truncations and point mutants are indicated by arrowheads
724 and closed circles, respectively. **(B)** Surface rendering of adjacent BTB domains from the crystal
725 structure of human KCTD5 [39]. Here and in subsequent figure panels, Inc residue numbers are
726 superimposed on conserved equivalents in KCTD5. Inc residues whose mutation specifically
727 weakens Inc-Cul3 associations are highlighted in magenta; other mutated residues are highlighted
728 in blue. **(C)** Ribbon rendering of adjacent KCTD5 BTB domains. Side chains are shown for Inc
729 residues mutated to assess Inc multimerization. Note that the T36A/D71A/R85E triple mutant
730 alters both faces of Inc. **(D)** Surface (left) and ribbon (right) rendering of human KCTD5. Inc C-
731 terminal point mutants are labeled and indicated in magenta; side chains are shown in the ribbon
732 rendering. Note that KCTD5 residues equivalent to Inc amino acids 186-211 are not resolved in
733 the crystal structure, suggesting that they are disordered.

734

735 **S2 Fig. Stability of Inc truncations in S2 cells**

736 **(A)** Immunoblot of lysates prepared from transiently transfected S2 cells treated with
737 cycloheximide (CHX) for indicated durations. **(B)** Quantitation of two biological replicates. For
738 all timepoints, Welch's ANOVA $p<0.05$ for comparison to wild-type Inc (1-211); Dunnett's tests;
739 $*p < 0.05$.

740

741 **S3 Fig. Interactions of Inc 1-156 and Inc 22-123 with Cul3**

742 **(A-B)** Co-immunoprecipitation of 3×Myc-tagged Inc 1-156 **(A)** or Inc 22-123 **(B)** with 3×FLAG-
743 Cul3 from transiently transfected S2 cells.

744

745

746 **S4 Fig. Stability of Inc point mutants in S2 cells**

747 **(A)** Immunoblot of lysates prepared from transiently transfected S2 cells treated with
748 cycloheximide (CHX) for indicated durations. **(B)** Quantitation of two biological replicates. For
749 all timepoints, Welch's ANOVA $p < 0.05$ for comparison to wild-type Inc.

750

751 **S5 Fig. Expression of Inc BTB domain point mutants in vivo**

752 Immunoblot of male whole animal lysates expressing 3×FLAG-tagged Inc and Inc point mutants
753 under *inc-Gal4* control. Animals are heterozygous for UAS transgenes.

754

755 **S6 Fig. Inc truncations and point mutants lack dominant negative activity in vivo**

756 Total daily sleep for animals expressing tagged Inc or Inc point mutants under the control of
757 *elav^{c155}-Gal4* **(A-C)** and *inc-Gal4* **(D)**. **(A)** *elav^{c155}-Gal4* expression of 3×FLAG-tagged Inc point
758 mutants. n = 5-24. **(B)** *elav^{c155}-Gal4* expression of 3×FLAG-tagged Inc truncations. n = 23-54. **(C)**
759 *elav^{c155}-Gal4* expression of Myc-tagged Inc point mutants. Note that Inc^{R135H} is statistically
760 indistinguishable from Inc and Inc^{AAA}. n = 18-32. **(D)** *inc-Gal4* expression of 3×FLAG-tagged
761 Myc-tagged Inc point mutants. n = 19-63; For all panels, mean ± SEM is shown. Kruskal-Wallis
762 and Dunn's tests; *$p < 0.01$; ns, not significant ($p > 0.05$). For all panels, animals are heterozygous
763 for UAS transgenes.

764

765 **S7 Fig. Additional sleep parameters for animals expressing Inc BTB domain point mutants**

766 **(A-D)** Sleep parameters for *inc^{1} inc-Gal4* animals expressing 3×FLAG-tagged Inc or Inc point
767 mutants. **(A)** Nighttime sleep. **(B)** Daytime sleep. **(C)** Sleep bout duration. **(D)** Sleep bout number.

768 Mean ± SEM is shown. n = 16-58 as in Fig 3B; Kruskal-Wallis and Dunn's tests; *p < 0.05; ***p
769 < 0.001; ****p < 0.0001; ns, not significant (p > 0.05). For all panels, animals are heterozygous
770 for UAS transgenes.
771
772 **S8 Fig. *UAS-Inc* transgenes do not alter sleep in *inc* mutants in the absence of Gal4**
773 Total daily sleep is shown for control, inc^1, and inc^1 animals heterozygous for indicated UAS
774 transgenes. Mean ± SEM is shown. n = 83-65; Kruskal-Wallis and Dunn's tests; ***p < 0.001; ns,
775 not significant (p > 0.05**).**
776
777 **S9 Fig. Additional sleep parameters for animals expressing Inc C-terminal truncations**
778 **(A-D)** Sleep parameters for inc^1 *inc-Gal4* animals expressing 3×FLAG-tagged Inc or C-terminally
779 truncated Inc mutants. **(A)** Nighttime sleep. **(B)** Daytime sleep. **(C)** Sleep bout duration. **(D)** Sleep
780 bout number. Mean ± SEM is shown. n = 27-30 as in Fig 4B; Kruskal-Wallis and Dunn's tests; *p
781 < 0.05; **p < 0.01; ****p < 0.0001; ns, not significant (p > 0.05). For all panels, animals are
782 heterozygous for UAS transgenes.
783
784 **S10 Fig. Additional sleep parameters for animals expressing Inc C-terminal point mutants**
785 **(A-D)** Sleep parameters for inc^1 *inc-Gal4* animals expressing 3×Myc-tagged Inc or Inc point
786 mutants. **(A)** Nighttime sleep. **(B)** Daytime sleep. **(C)** Sleep bout duration. **(D)** Sleep bout number.
787 Mean ± SEM is shown. n = 24-45 as in Fig 6E; Kruskal-Wallis, p<0.0001 and Dunn's tests; *p <
788 0.05; ***p < 0.001; ****p < 0.0001; ns, not significant (p > 0.05). For all panels, animals are
789 heterozygous for UAS transgenes.
790
791 **S1 Table. Summary of Inc point mutants targeting Inc-Cul3 interactions**

792 **(PDF)**

793

794 **S2 Table. Summary of Inc point mutants targeting Inc-Inc interactions**

795 **(PDF)**

796 **References**

797 1. Codina-Solà M, Rodríguez-Santiago B, Homs A, Santoyo J, Rigau M, Aznar-Laín G, et al.
798 Integrated analysis of whole-exome sequencing and transcriptome profiling in males with
799 autism spectrum disorders. Mol Autism. 2015;6: 21. doi:10.1186/s13229-015-0017-0

800 2. da Silva Montenegro EM, Costa CS, Campos G, Scliar M, de Almeida TF, Zachi EC, et al.
801 Meta-Analyses Support Previous and Novel Autism Candidate Genes: Outcomes of an
802 Unexplored Brazilian Cohort. Autism Research. 2020;13: 199–206. doi:10.1002/aur.2238

803 3. De Rubeis S, He X, Goldberg AP, Poultney CS, Samocha K, Cicek AE, et al. Synaptic,
804 transcriptional and chromatin genes disrupted in autism. Nature. 2014;515: 209–215.
805 doi:10.1038/nature13772

806 4. Iwafuchi S, Kikuchi A, Endo W, Inui T, Aihara Y, Satou K, et al. A novel stop-gain CUL3
807 mutation in a Japanese patient with autism spectrum disorder. Brain and Development.
808 2021;43: 303–307. doi:10.1016/j.braindev.2020.09.015

809 5. Kong A, Frigge ML, Masson G, Besenbacher S, Sulem P, Magnusson G, et al. Rate of de
810 novo mutations and the importance of father's age to disease risk. Nature. 2012;488:
811 471–475. doi:10.1038/nature11396

812 6. O'Roak BJ, Vives L, Girirajan S, Karakoc E, Krumm N, Coe BP, et al. Sporadic autism
813 exomes reveal a highly interconnected protein network of de novo mutations. Nature.
814 2012;485: 246–250. doi:10.1038/nature10989

815 7. Wang T, Guo H, Xiong B, Stessman HAF, Wu H, Coe BP, et al. De novo genic mutations
816 among a Chinese autism spectrum disorder cohort. Nat Comms. 2016;7: 13316.
817 doi:10.1038/ncomms13316

818 8. Amar M, Pramod AB, Yu N-K, Herrera VM, Qiu LR, Moran-Losada P, et al. Autism-linked
819 Cullin3 germline haploinsufficiency impacts cytoskeletal dynamics and cortical
820 neurogenesis through RhoA signaling. Mol Psychiatry. 2021;26: 3586–3613.
821 doi:10.1038/s41380-021-01052-x

822 9. Dong Z, Chen W, Chen C, Wang H, Cui W, Tan Z, et al. CUL3 Deficiency Causes Social
823 Deficits and Anxiety-like Behaviors by Impairing Excitation-Inhibition Balance through the
824 Promotion of Cap-Dependent Translation. Neuron. 2020;105: 475-490.e6.
825 doi:10.1016/j.neuron.2019.10.035

826 10. Morandell J, Schwarz LA, Basilico B, Tasciyan S, Dimchev G, Nicolas A, et al. Cul3
827 regulates cytoskeleton protein homeostasis and cell migration during a critical window of
828 brain development. Nat Comms. 2021;12: 3058–22. doi:10.1038/s41467-021-23123-x

829 11. Rapanelli M, Tan T, Wang W, Wang X, Wang Z-J, Zhong P, et al. Behavioral, circuitry, and
830 molecular aberrations by region-specific deficiency of the high-risk autism gene Cul3.
831 Molecular Psychiatry. 2019;22: 345–14. doi:10.1038/s41380-019-0498-x

832 12. Rapanelli M. Cholinergic neurons in the basal forebrain are involved in behavioral
833 abnormalities associated with Cul3 deficiency: Role of prefrontal cortex projections in
834 cognitive deficits. Translational Psychiatry. 2023.

835 13. Xia Q, Walker AK, Song C, Wang J, Singh A, Mobley JA, et al. Effects of heterozygous
836 deletion of autism-related gene Cullin-3 in mice. Li Y, editor. PLoS ONE. 2023;18:
837 e0283299. doi:10.1371/journal.pone.0283299

838 14. Gao N, Liu Z, Wang H, Shen C, Dong Z, Cui W, et al. Deficiency of Cullin 3, a Protein
839 Encoded by a Schizophrenia and Autism Risk Gene, Impairs Behaviors by Enhancing the
840 Excitability of Ventral Tegmental Area (VTA) DA Neurons. J Neurosci. 2023;43: 6249–
841 6267. doi:10.1523/JNEUROSCI.0247-23.2023

842 15. Zhu S, Perez R, Pan M, Lee T. Requirement of Cul3 for axonal arborization and dendritic
843 elaboration in Drosophila mushroom body neurons. Journal of Neuroscience. 2005;25:
844 4189–4197. doi:10.1523/JNEUROSCI.0149-05.2005

845 16. Schaefer H, Rongo C. KEL-8 is a substrate receptor for CUL3-dependent ubiquitin ligase
846 that regulates synaptic glutamate receptor turnover. Mol Biol Cell. 2006;17: 1250–1260.
847 doi:10.1091/mbc.E05-08-0794

848 17. Stavropoulos N, Young MW. insomniac and Cullin-3 regulate sleep and wakefulness in
849 Drosophila. Neuron. 2011;72: 964–976. doi:10.1016/j.neuron.2011.12.003

850 18. Pfeiffenberger C, Allada R. Cul3 and the BTB adaptor insomniac are key regulators of sleep
851 homeostasis and a dopamine arousal pathway in Drosophila. PLoS Genet. 2012;8:
852 e1003003. doi:10.1371/journal.pgen.1003003

853 19. Singh K, Ju JY, Walsh MB, DiIorio MA, Hart AC. Deep conservation of genes required for
854 both Drosphila melanogaster and Caenorhabditis elegans sleep includes a role for
855 dopaminergic signaling. Sleep. 2014;37: 1439–1451. doi:10.5665/sleep.3990

856 20. Kikuma K, Li X, Perry S, Li Q, Goel P, Chen C, et al. Cul3 and insomniac are required for
857 rapid ubiquitination of postsynaptic targets and retrograde homeostatic signaling. Nat
858 Comms. 2019;10: 2998–13. doi:10.1038/s41467-019-10992-6

859 21. Furukawa M, He YJ, Borchers C, Xiong Y. Targeting of protein ubiquitination by BTB-
860 Cullin 3-Roc1 ubiquitin ligases. Nat Cell Biol. 2003;5: 1001–1007. doi:10.1038/ncb1056

861 22. Geyer R, Wee S, Anderson S, Yates J, Wolf DA. BTB/POZ domain proteins are putative
862 substrate adaptors for cullin 3 ubiquitin ligases. Mol Cell. 2003;12: 783–790.

863 23. Pintard L, Willis JH, Willems A, Johnson J-LF, Srayko M, Kurz T, et al. The BTB protein
864 MEL-26 is a substrate-specific adaptor of the CUL-3 ubiquitin-ligase. Nature. 2003;425:
865 311–316. doi:10.1038/nature01959

866 24. Xu L, Wei Y, Reboul J, Vaglio P, Shin T-H, Vidal M, et al. BTB proteins are substrate-
867 specific adaptors in an SCF-like modular ubiquitin ligase containing CUL-3. Nature.
868 2003;425: 316–321. doi:10.1038/nature01985

869 25. Bennett EJ, Rush J, Gygi SP, Harper JW. Dynamics of cullin-RING ubiquitin ligase network
870 revealed by systematic quantitative proteomics. Cell. 2010;143: 951–965.
871 doi:10.1016/j.cell.2010.11.017

872 26. Allen E, Ding J, Wang W, Pramanik S, Chou J, Yau V, et al. Gigaxonin-controlled
873 degradation of MAP1B light chain is critical to neuronal survival. Nature. 2005;438: 224–
874 228.

875 27. Salinas GD, Blair LAC, Needleman LA, Gonzales JD, Chen Y, Li M, et al. Actinfilin is a
876 Cul3 substrate adaptor, linking GluR6 kainate receptor subunits to the ubiquitin-proteasome
877 pathway. J Biol Chem. 2006;281: 40164–40173. doi:10.1074/jbc.M608194200

878 28. Zhang Q, Zhang L, Wang B, Ou C-Y, Chien C-T, Jiang J. A hedgehog-induced BTB protein
879 modulates hedgehog signaling by degrading Ci/Gli transcription factor. Dev Cell. 2006;10:
880 719–729. doi:10.1016/j.devcel.2006.05.004

881 29. Sobieszczuk DF, Poliakov A, Xu Q, Wilkinson DG. A feedback loop mediated by
882 degradation of an inhibitor is required to initiate neuronal differentiation. Genes Dev.
883 2010;24: 206–218. doi:10.1101/gad.554510

884 30. Lin M-Y, Lin Y-M, Kao T, Chuang H-H, Chen R-H. PDZ-RhoGEF ubiquitination by
885 Cullin3-KLHL20 controls neurotrophin-induced neurite outgrowth. J Cell Biol. 2011;193:
886 985–994. doi:10.1083/jcb.201103015

887 31. Tseng LA, Bixby JL. Interaction of an intracellular pentraxin with a BTB-Kelch protein is
888 associated with ubiquitylation, aggregation and neuronal apoptosis. Mol Cell Neurosci.
889 2011;47: 254–264. doi:10.1016/j.mcn.2011.04.005

890 32. Escamilla CO, Filonova I, Walker AK, Xuan ZX, Holehonnur R, Espinosa F, et al. Kctd13
891 deletion reduces synaptic transmission via increased RhoA. Nature. 2017;551: 227–231.
892 doi:10.1038/nature24470

893 33. Li Q, Kellner DA, Hatch HAM, Yumita T, Sanchez S, Machold RP, et al. Conserved
894 properties of Drosophila Insomniac link sleep regulation and synaptic function. PLoS
895 Genet. 2017;13: e1006815. doi:10.1371/journal.pgen.1006815

896 34. Mathew R, Seiler MP, Scanlon ST, Mao A-P, Constantinides MG, Bertozzi-Villa C, et al.
897 BTB-ZF factors recruit the E3 ligase cullin 3 to regulate lymphoid effector programs.
898 Nature. 2012. doi:10.1038/nature11548

899 35. Schwenk J, Metz M, Zolles G, Turecek R, Fritzius T, Bildl W, et al. Native GABA(B)
900 receptors are heteromultimers with a family of auxiliary subunits. Nature. 2010;465: 231–
901 235. doi:10.1038/nature08964

902 36. Stogios PJ, Downs GS, Jauhal JJS, Nandra SK, Privé GG. Sequence and structural analysis
903 of BTB domain proteins. Genome Biol. 2005;6: R82. doi:10.1186/gb-2005-6-10-r82

904 37. Mencacci NE, Rubio-Agusti I, Zdebik A, Asmus F, Ludtmann MHR, Ryten M, et al. A
905 missense mutation in KCTD17 causes autosomal dominant myoclonus-dystonia. American
906 journal of human genetics. 2015;96: 938–947. doi:10.1016/j.ajhg.2015.04.008

907 38. Bayón Y, Trinidad AG, de la Puerta ML, Del Carmen Rodríguez M, Bogetz J, Rojas A, et al.
908 KCTD5, a putative substrate adaptor for cullin3 ubiquitin ligases. FEBS J. 2008;275: 3900–
909 3910. doi:10.1111/j.1742-4658.2008.06537.x

910 39. Dementieva IS, Tereshko V, McCrossan ZA, Solomaha E, Araki D, Xu C, et al. Pentameric
911 assembly of potassium channel tetramerization domain-containing protein 5. J Mol Biol.
912 2009;387: 175–191. doi:10.1016/j.jmb.2009.01.030

913 40. Errington WJ, Khan MQ, Bueler SA, Rubinstein JL, Chakrabartty A, Privé GG. Adaptor
914 protein self-assembly drives the control of a cullin-RING ubiquitin ligase. Structure.
915 2012;20: 1141–1153. doi:10.1016/j.str.2012.04.009

916 41. Canning P, Cooper CDO, Krojer T, Murray JW, Pike ACW, Chaikuad A, et al. Structural
917 basis for Cul3 protein assembly with the BTB-Kelch family of E3 ubiquitin ligases. J Biol
918 Chem. 2013;288: 7803–7814. doi:10.1074/jbc.M112.437996

919 42. Ji AX, Privé GG. Crystal Structure of KLHL3 in Complex with Cullin3. PLoS ONE. 2013;8:
920 e60445. doi:10.1371/journal.pone.0060445

921 43. Balasco N, Pirone L, Smaldone G, Di Gaetano S, Esposito L, Pedone EM, et al. Molecular
922 recognition of Cullin3 by KCTDs: insights from experimental and computational
923 investigations. Biochim Biophys Acta. 2014;1844: 1289–1298.
924 doi:10.1016/j.bbapap.2014.04.006

925 44. Pirone L, Smaldone G, Esposito C, Balasco N, Petoukhov MV, Spilotros A, et al. Proteins
926 involved in sleep homeostasis: Biophysical characterization of INC and its partners.
927 Biochimie. 2016;131: 106–114. doi:10.1016/j.biochi.2016.09.013

928 45. Ji AX, Chu A, Nielsen TK, Benlekbir S, Rubinstein JL, Privé GG. Structural insights into
929 KCTD protein assembly and Cullin3 recognition. J Mol Biol. 2015.
930 doi:10.1016/j.jmb.2015.08.019

931 46. Frank CA, Kennedy MJ, Goold CP, Marek KW, Davis GW. Mechanisms underlying the
932 rapid induction and sustained expression of synaptic homeostasis. Neuron. 2006;52: 663–
933 677. doi:10.1016/j.neuron.2006.09.029

934 47. Pintard L, Kurz T, Glaser S, Willis JH, Peter M, Bowerman B. Neddylation and
935 deneddylation of CUL-3 is required to target MEI-1/Katanin for degradation at the meiosis-
936 to-mitosis transition in C. elegans. Curr Biol. 2003;13: 911–921.

937 48. Wee S, Geyer RK, Toda T, Wolf DA. CSN facilitates Cullin-RING ubiquitin ligase function
938 by counteracting autocatalytic adapter instability. Nat Cell Biol. 2005;7: 387–391.
939 doi:10.1038/ncb1241

940 49. Zhang DD, Lo S-C, Sun Z, Habib GM, Lieberman MW, Hannink M. Ubiquitination of
941 Keap1, a BTB-Kelch substrate adaptor protein for Cul3, targets Keap1 for degradation by a
942 proteasome-independent pathway. J Biol Chem. 2005;280: 30091–30099.
943 doi:10.1074/jbc.M501279200

944 50. Tener SJ, Lin Z, Park SJ, Oraedu K, Ulgherait M, Van Beek E, et al. Neuronal knockdown of
945 Cullin3 as a Drosophila model of autism spectrum disorder. Sci Rep. 2024;14: 1541.
946 doi:10.1038/s41598-024-51657-9

947 51. Pinkas DM, Sanvitale CE, Bufton JC, Sorrell FJ, Solcan N, Chalk R, et al. Structural
948 complexity in the KCTD family of Cullin3-dependent E3 ubiquitin ligases. Biochem J.
949 2017;474: 3747–3761. doi:10.1042/BCJ20170527

950 52. Jiang W, Wang W, Kong Y, Zheng S. Structural basis for the ubiquitination of G protein βγ
951 subunits by KCTD5/Cullin3 E3 ligase. Sci Adv. 2023;9: eadg8369.
952 doi:10.1126/sciadv.adg8369

953 53. Nguyen DM, Rath DH, Devost D, Pétrin D, Rizk R, Ji AX, et al. Structure and dynamics of a
954 pentameric KCTD5/Cullin3/Gβγ E3 ubiquitin ligase complex.
955 http://biorxiv.org/lookup/doi/10.1101/2023.09.20.558662; 2023 Sep.
956 doi:10.1101/2023.09.20.558662

957 54. McGourty CA, Akopian D, Walsh C, Gorur A, Werner A, Schekman R, et al. Regulation of
958 the CUL3 Ubiquitin Ligase by a Calcium-Dependent Co-adaptor. Cell. 2016;167: 525-
959 538.e14. doi:10.1016/j.cell.2016.09.026

960 55. Muntean BS, Marwari S, Li X, Sloan DC, Young BD, Wohlschlegel JA, et al. Members of
961 the KCTD family are major regulators of cAMP signaling. Proceedings of the National
962 Academy of Sciences. 2022;119. doi:10.1073/pnas.2119237119

963 56. Li Q, Jang H, Lim KY, Lessing A, Stavropoulos N. insomniac links the development and
964 function of a sleep-regulatory circuit. Calabrese RL, Cirelli C, editors. eLife. 2021;10:
965 e65437. doi:10.7554/eLife.65437

966 57. Kim E-J, Kim S-H, Jin X, Jin X, Kim H. KCTD2, an adaptor of Cullin3 E3 ubiquitin ligase,
967 suppresses gliomagenesis by destabilizing c-Myc. Cell Death Differ. 2017;24: 649–659.
968 doi:10.1038/cdd.2016.151

969 58. He H, Peng Y, Fan S, Chen Y, Zheng X, Li C. Cullin3/KCTD5 induces monoubiquitination
970 of ΔNp63α and impairs its activity. FEBS Letters. 2018;592: 2334–2340.
971 doi:10.1002/1873-3468.13104

972 59. Cho HJ, Ryu K-J, Baek KE, Lim J, Kim T, Song CY, et al. Cullin 3/KCTD5 promotes the
973 ubiqutination of Rho guanine nucleotide dissociation inhibitor 1 and regulates its stability. J
974 Microbiol Biotechnol. 2020;30: 1–7. doi:10.4014/jmb.2007.07033

975 60. Brockmann M, Blomen VA, Nieuwenhuis J, Stickel E, Raaben M, Bleijerveld OB, et al.
976 Genetic wiring maps of single-cell protein states reveal an off-switch for GPCR signalling.
977 Nature. 2017;546: 307–311. doi:10.1038/nature22376

978 61. Young BD, Sha J, Vashisht AA, Wohlschlegel JA. Human Multisubunit E3 Ubiquitin Ligase
979 Required for Heterotrimeric G-Protein β-Subunit Ubiquitination and Downstream
980 Signaling. J Proteome Res. 2021. doi:10.1021/acs.jproteome.1c00292

981 62. Kasahara K, Kawakami Y, Kiyono T, Yonemura S, Kawamura Y, Era S, et al. Ubiquitin-
982 proteasome system controls ciliogenesis at the initial step of axoneme extension. Nat
983 Comms. 2014;5: 5081. doi:10.1038/ncomms6081

984 63. Kim K, Ryu D, Dongiovanni P, Ozcan L, Nayak S, Ueberheide B, et al. Degradation of
985 PHLPP2 by KCTD17, via a Glucagon-Dependent Pathway, Promotes Hepatic Steatosis.
986 Gastroenterology. 2017;153: 1568-1580.e10. doi:10.1053/j.gastro.2017.08.039

987 64. Shin MC, Jung YH, Jeong Y, Oh A-R, Lee SB, Kim K. Kctd17-mediated Chop degradation
988 promotes adipogenic differentiation. Biochemical and Biophysical Research
989 Communications. 2023;653: 126–132. doi:10.1016/j.bbrc.2023.02.068

990 65. Boada M, Antúnez C, Ramírez-Lorca R, DeStefano AL, González-Pérez A, Gayán J, et al.
991 ATP5H/KCTD2 locus is associated with Alzheimer's disease risk. Molecular
992 Psychiatry. 2014;19: 682–687. doi:10.1038/mp.2013.86

993 66. Barfield R, Wang H, Liu Y, Brody JA, Swenson B, Li R, et al. Epigenome-wide association
994 analysis of daytime sleepiness in the Multi-Ethnic Study of Atherosclerosis reveals African-
995 American-specific associations. Sleep. 2019;42: zsz101. doi:10.1093/sleep/zsz101

996 67. Lin DM, Goodman CS. Ectopic and increased expression of Fasciclin II alters motoneuron
997 growth cone guidance. Neuron. 1994;13: 507–523.

998 68. Budnik V, Koh Y-H, Guan B, Hartmann B, Hough C, Woods D, et al. Regulation of Synapse
999 Structure and Function by the Drosophila Tumor Suppressor Gene dlg. Neuron. 1996;17:
1000 627–640. doi:10.1016/S0896-6273(00)80196-8

1001 69. Hudson AM, Cooley L. Drosophila Kelch functions with Cullin-3 to organize the ring canal
1002 actin cytoskeleton. J Cell Biol. 2010;188: 29–37. doi:10.1083/jcb.200909017

1003 70. Groth AC, Fish M, Nusse R, Calos MP. Construction of transgenic Drosophila by using the
1004 site-specific integrase from phage phiC31. Genetics. 2004;166: 1775–1782.

1005 71. Ryder E, Blows F, Ashburner M, Bautista-Llacer R, Coulson D, Drummond J, et al. The
1006 DrosDel collection: a set of P-element insertions for generating custom chromosomal
1007 aberrations in Drosophila melanogaster. Genetics. 2004;167: 797–813.
1008 doi:10.1534/genetics.104.026658

1009

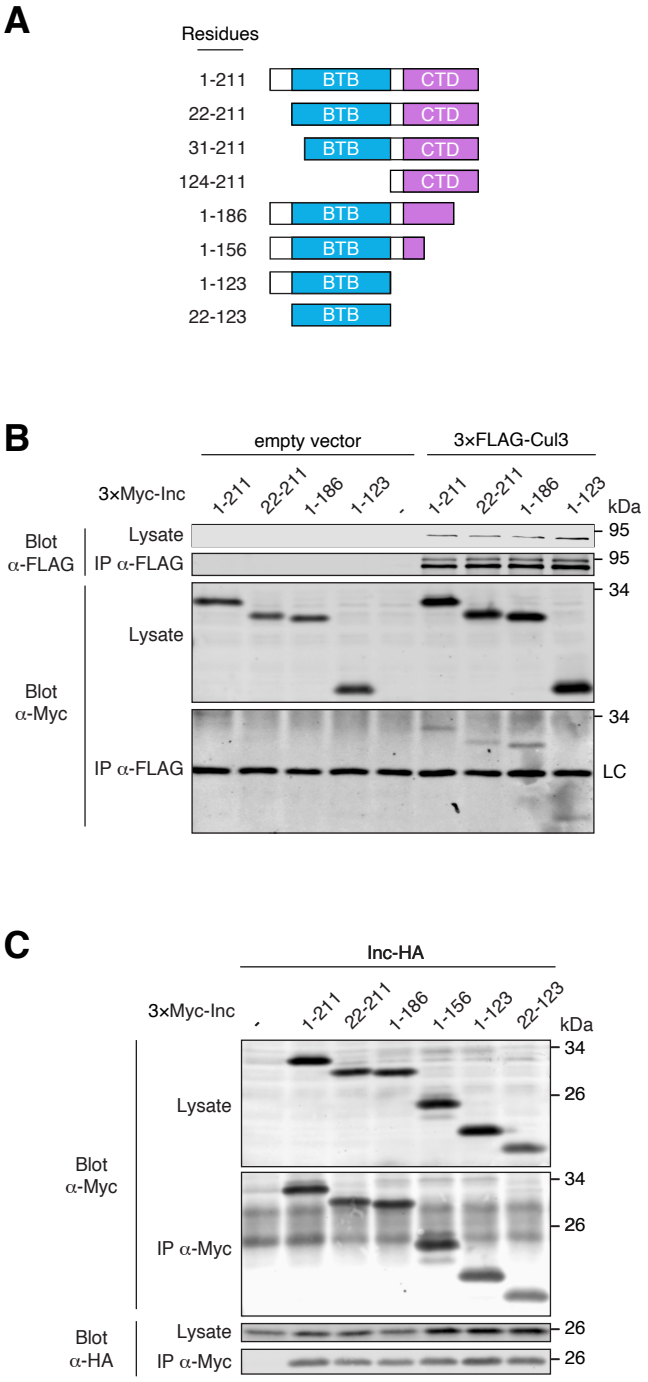
A
Residues
1-211
22-211
31-211
124-211
1-186
1-156
1-123
22-123
BTB
CTD
B
empty vector
3×FLAG-Cul3
3×Myc-Inc
1-211
22-211
1-186
1-123
-
kDa
Blot α-FLAG
Lysate
IP α-FLAG
95
Blot α-Myc
34
LC
C
Inc-HA
1-156
26
Blot α-HA

Figure 1

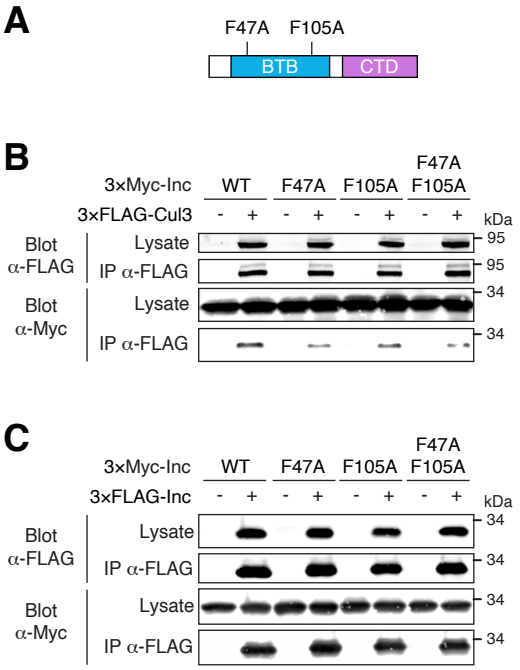
A
F47A
F105A
BTB
CTD
B
3×Myc-Inc
WT
F47A
F105A
F47A F105A
3×FLAG-Cul3
- + - + - + - +
kDa
Blot α-FLAG
Lysate
IP α-FLAG
95
95
Blot α-Myc
Lysate
IP α-FLAG
34
34
C
3×Myc-Inc
WT
F47A
F105A
F47A F105A
3×FLAG-Inc
- + - + - + - +
kDa
Blot α-FLAG
Lysate
IP α-FLAG
34
34
Blot α-Myc
Lysate
IP α-FLAG
34
34

Figure 2

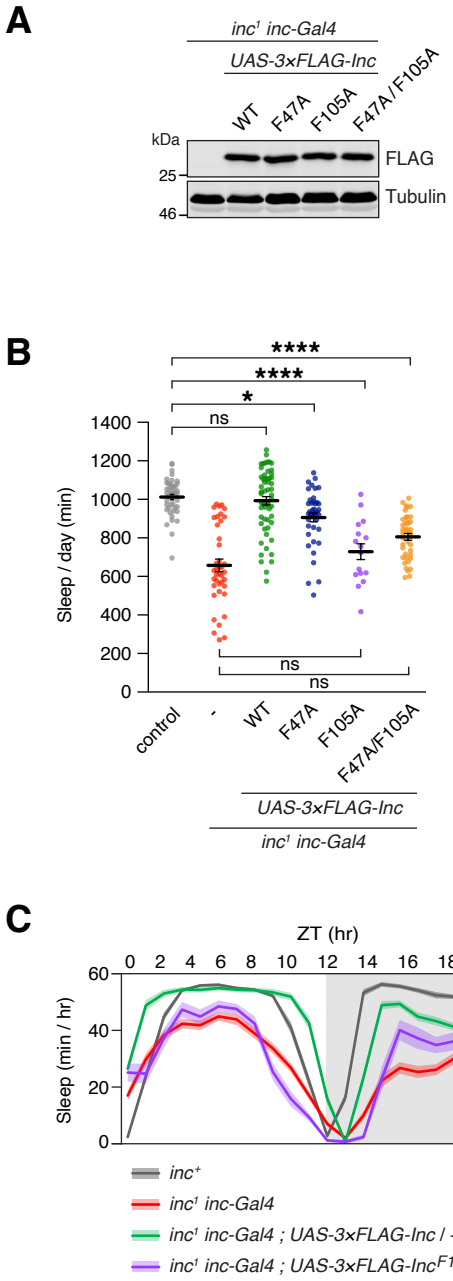
A
inc¹ inc-Gal4
UAS-3xFLAG-Inc
WT
F47A
F105A
F47A / F105A
kDa
25
46
FLAG
Tubulin
B
****
****
*
ns
1400
1200
1000
800
600
400
200
0
Sleep / day (min)
ns
ns
control
-
WT
F47A
F105A
F47A/F105A
UAS-3xFLAG-Inc
inc¹ inc-Gal4
C
ZT (hr)
0 2 4 6 8 10 12 14 16 18 20 22
60
40
20
0
Sleep (min / hr)
inc⁺
inc¹ inc-Gal4
inc¹ inc-Gal4 ; UAS-3xFLAG-Inc / +
inc¹ inc-Gal4 ; UAS-3xFLAG-Inc^F105A / +

Figure 3

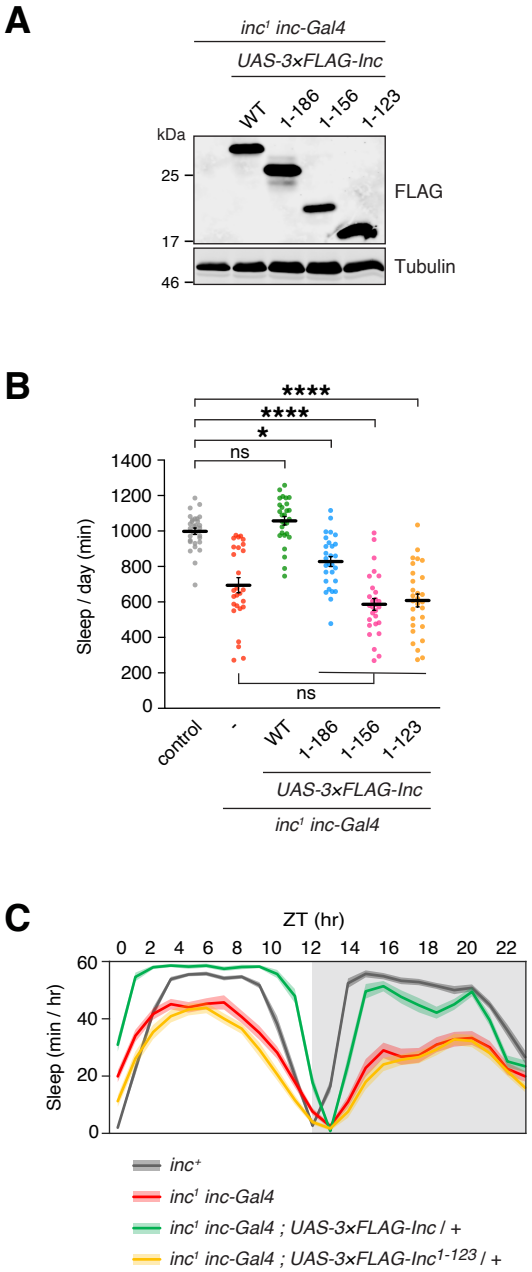
A
inc¹ inc-Gal4
UAS-3xFLAG-Inc
WT
1-186
1-156
1-123
kDa
25
17
46
FLAG
Tubulin
B
****
****
*
ns
ns
Sleep / day (min)
1400
1200
1000
800
600
400
200
0
control
-
WT
1-186
1-156
1-123
UAS-3xFLAG-Inc
inc¹ inc-Gal4
C
ZT (hr)
0 2 4 6 8 10 12 14 16 18 20 22
Sleep (min / hr)
60
40
20
0
inc⁺
inc¹ inc-Gal4
inc¹ inc-Gal4 ; UAS-3xFLAG-Inc / +
inc¹ inc-Gal4 ; UAS-3xFLAG-Inc1-123 / +

Figure 4

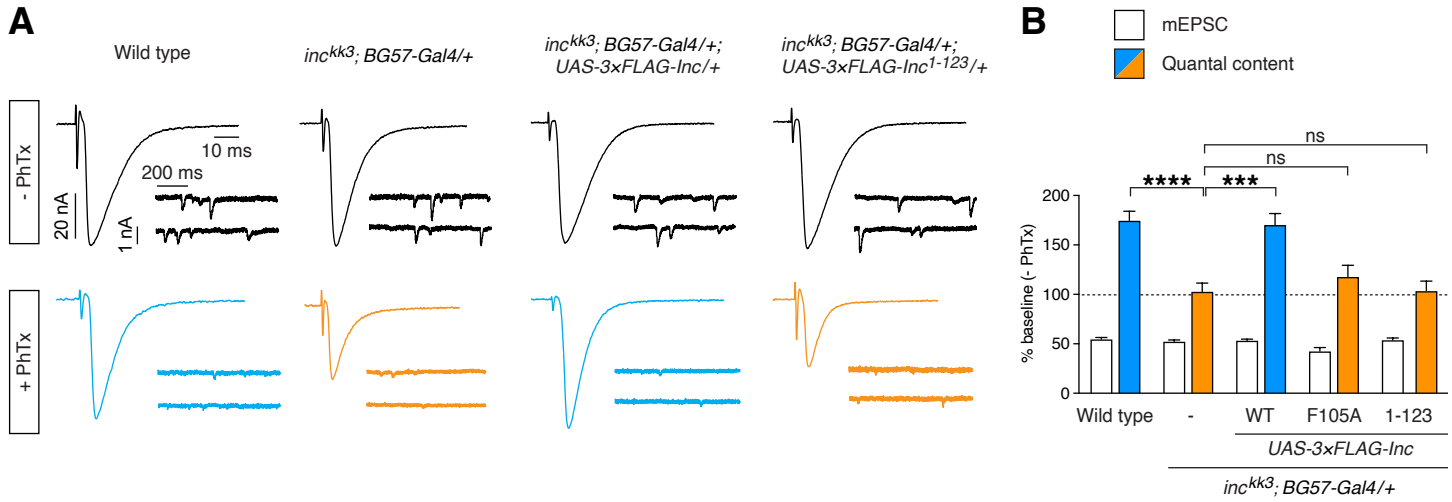
A
Wild type
inc^kk3; BG57-Gal4/+
inc^kk3; BG57-Gal4/+; UAS-3xFLAG-Inc/+
inc^kk3; BG57-Gal4/+; UAS-3xFLAG-Inc^1-123/+
- PhTx
+ PhTx
10 ms
200 ms
20 nA
1 nA
B
mEPSC
Quantal content
% baseline (- PhTx)
200
150
100
50
0
****
***
ns
ns
Wild type
-
WT
F105A
1-123
UAS-3xFLAG-Inc
inc^kk3; BG57-Gal4/+

Figure 5

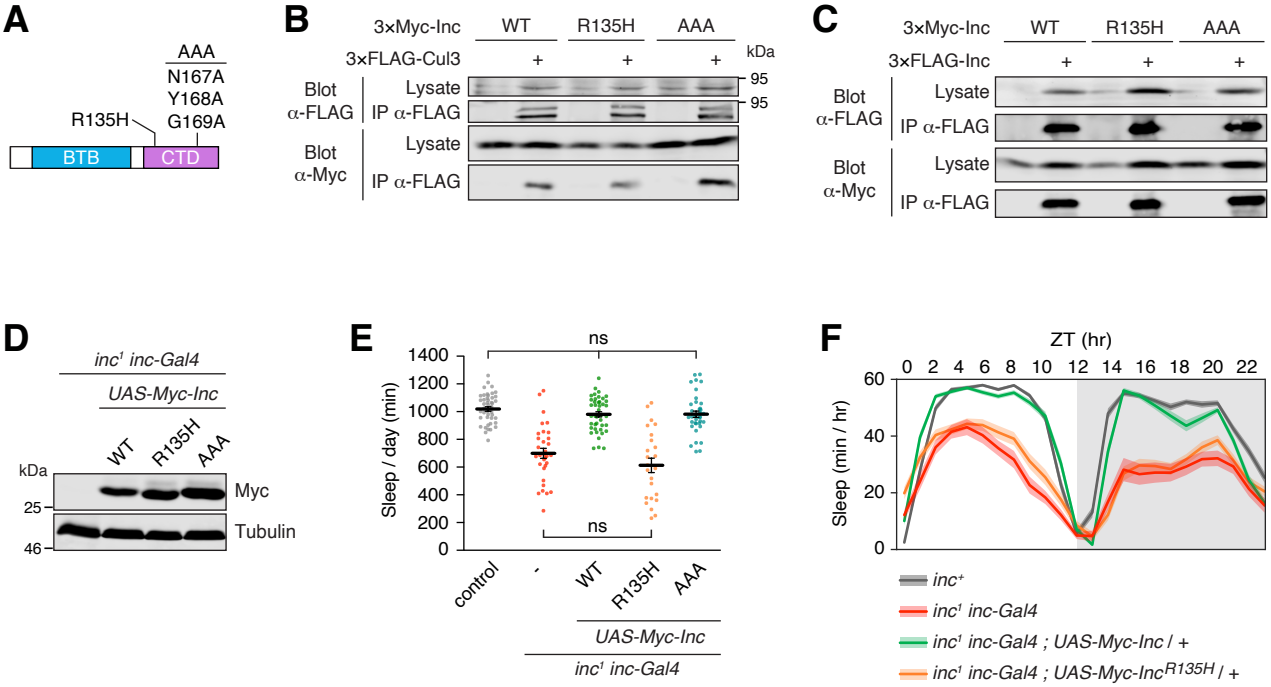
A
AAA
N167A
Y168A
G169A
R135H
BTB
CTD
B
3×Myc-Inc
WT
R135H
AAA
3×FLAG-Cul3
+
+
+
kDa
95
95
Blot α-FLAG
Lysate
IP α-FLAG
Blot α-Myc
Lysate
IP α-FLAG
C
3×Myc-Inc
WT
R135H
AAA
3×FLAG-Inc
+
+
+
Blot α-FLAG
Lysate
IP α-FLAG
Blot α-Myc
Lysate
IP α-FLAG
D
inc¹ inc-Gal4
UAS-Myc-Inc
WT
R135H
AAA
kDa
25
46
Myc
Tubulin
E
ns
ns
Sleep / day (min)
1400
1200
1000
800
600
400
200
0
control
-
WT
R135H
AAA
UAS-Myc-Inc
inc¹ inc-Gal4
F
ZT (hr)
0 2 4 6 8 10 12 14 16 18 20 22
Sleep (min / hr)
60
40
20
0
inc⁺
inc¹ inc-Gal4
inc¹ inc-Gal4 ; UAS-Myc-Inc / +
inc¹ inc-Gal4 ; UAS-Myc-Inc^R135H / +

Figure 6

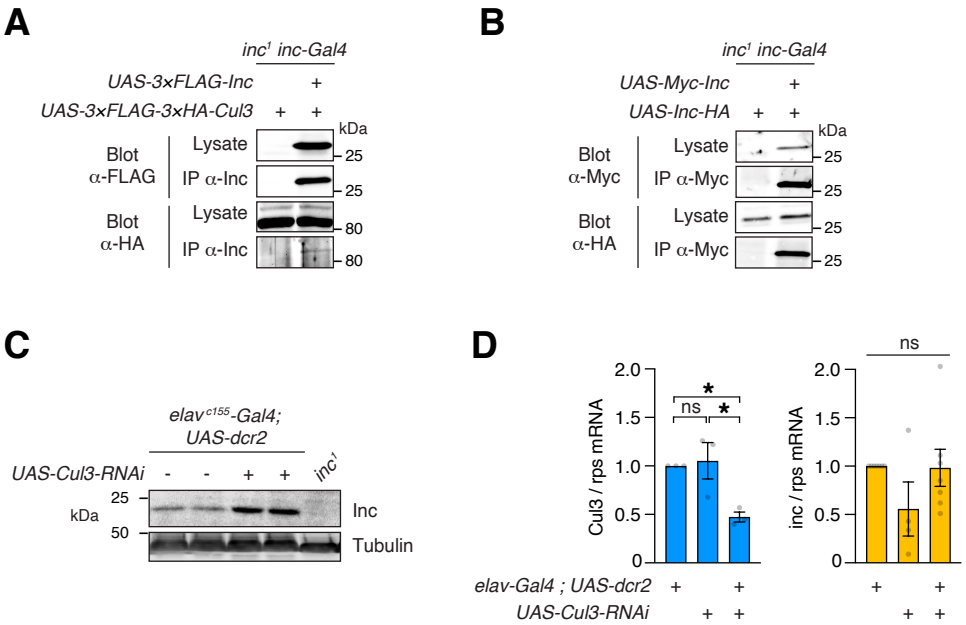
A
inc¹ inc-Gal4
UAS-3×FLAG-Inc +
UAS-3×FLAG-3×HA-Cul3 + +
kDa
Blot α-FLAG
Lysate
IP α-Inc
25
25
Blot α-HA
Lysate
IP α-Inc
80
80
B
inc¹ inc-Gal4
UAS-Myc-Inc +
UAS-Inc-HA + +
kDa
Blot α-Myc
Lysate
IP α-Myc
25
25
Blot α-HA
Lysate
IP α-Myc
25
25
C
elavc155-Gal4; UAS-dcr2
UAS-Cul3-RNAi - - + + inc¹
kDa
25
50
Inc
Tubulin
D
Cul3 / rps mRNA
2.0
1.5
1.0
0.5
0
ns
*
*
inc / rps mRNA
ns
elav-Gal4 ; UAS-dcr2 + + + +
UAS-Cul3-RNAi + + + +

Figure 7

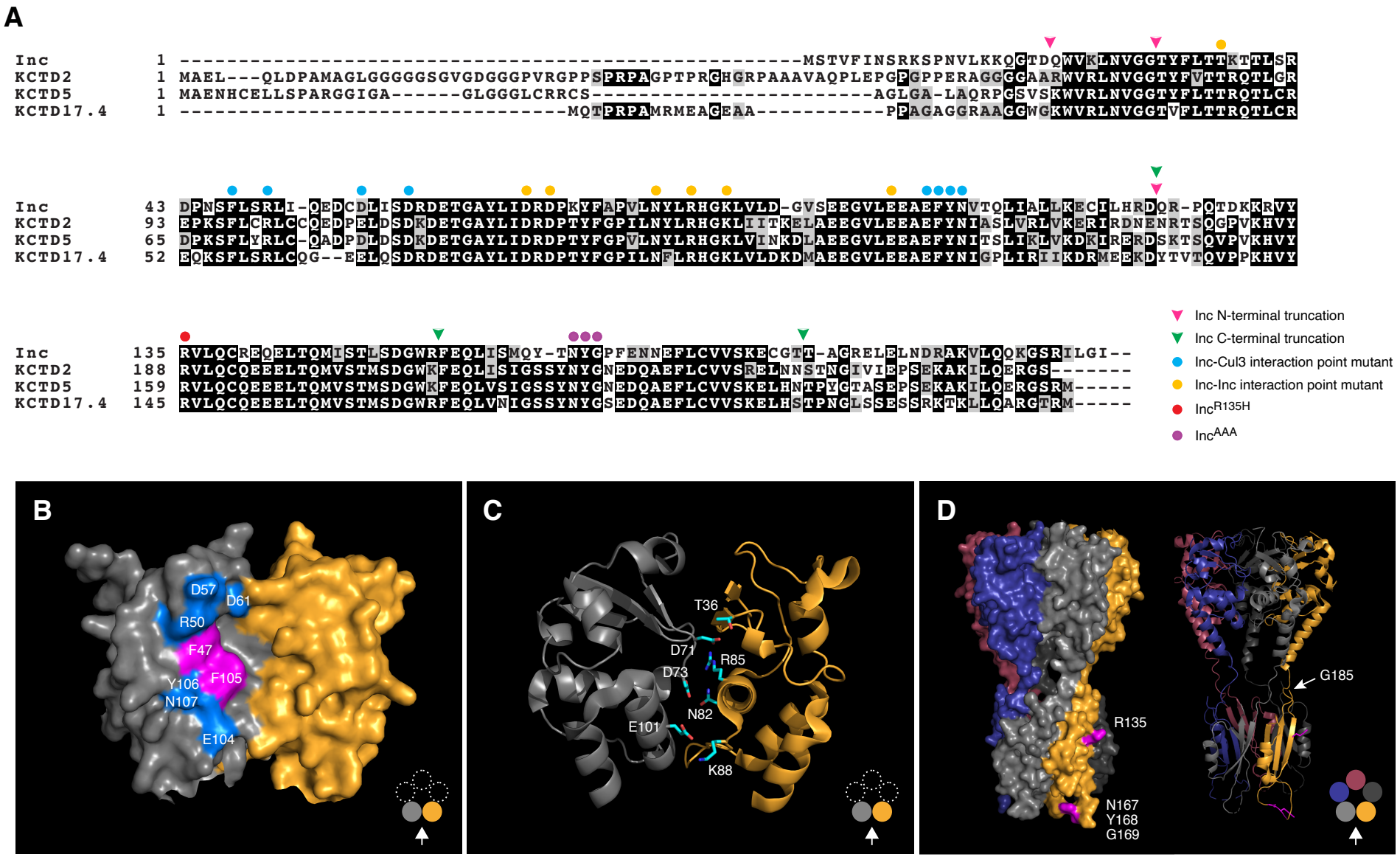

Supplementary Figure 1

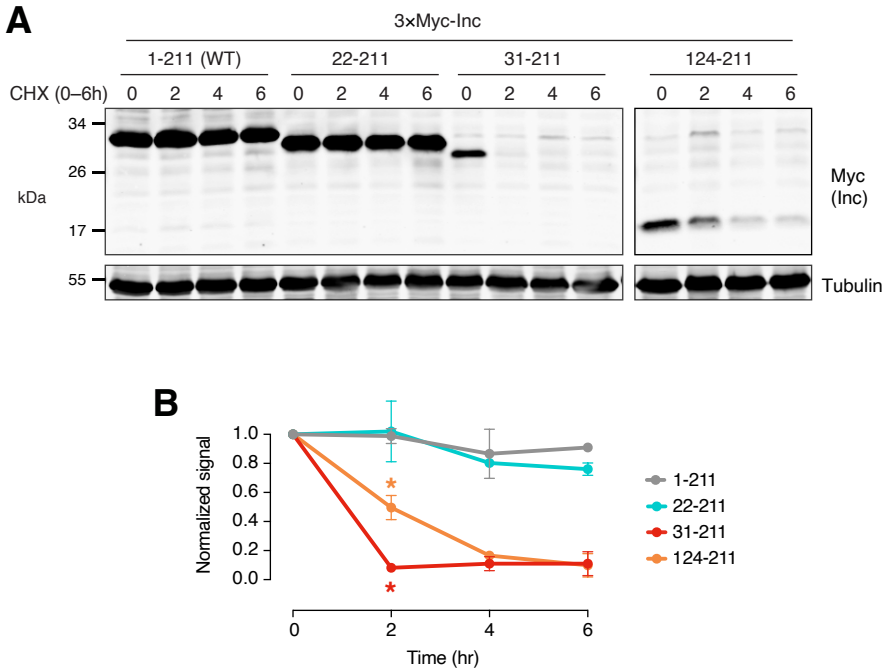

Supplementary Figure 2

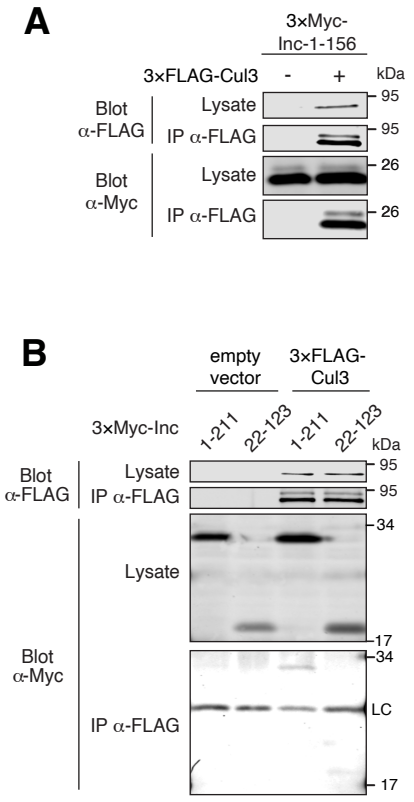

Supplementary Figure 3

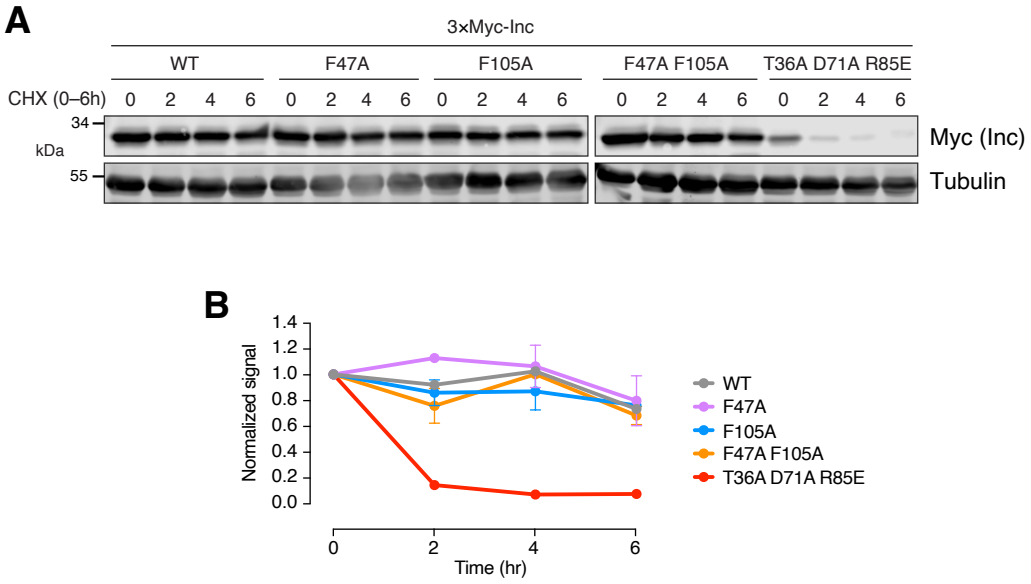

Supplementary Figure 4

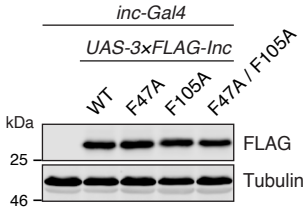

Supplementary Figure 5

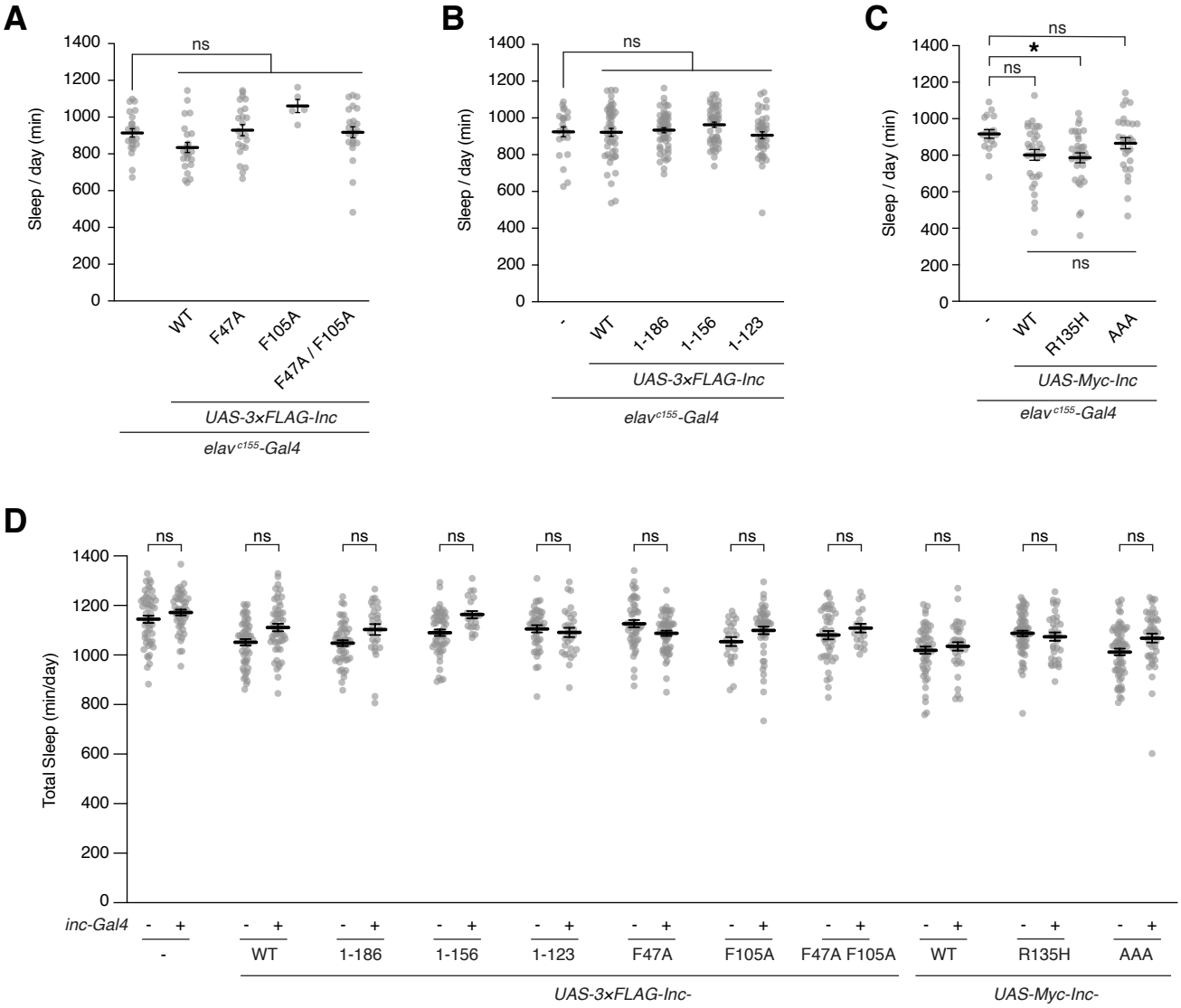

Supplementary Figure 6

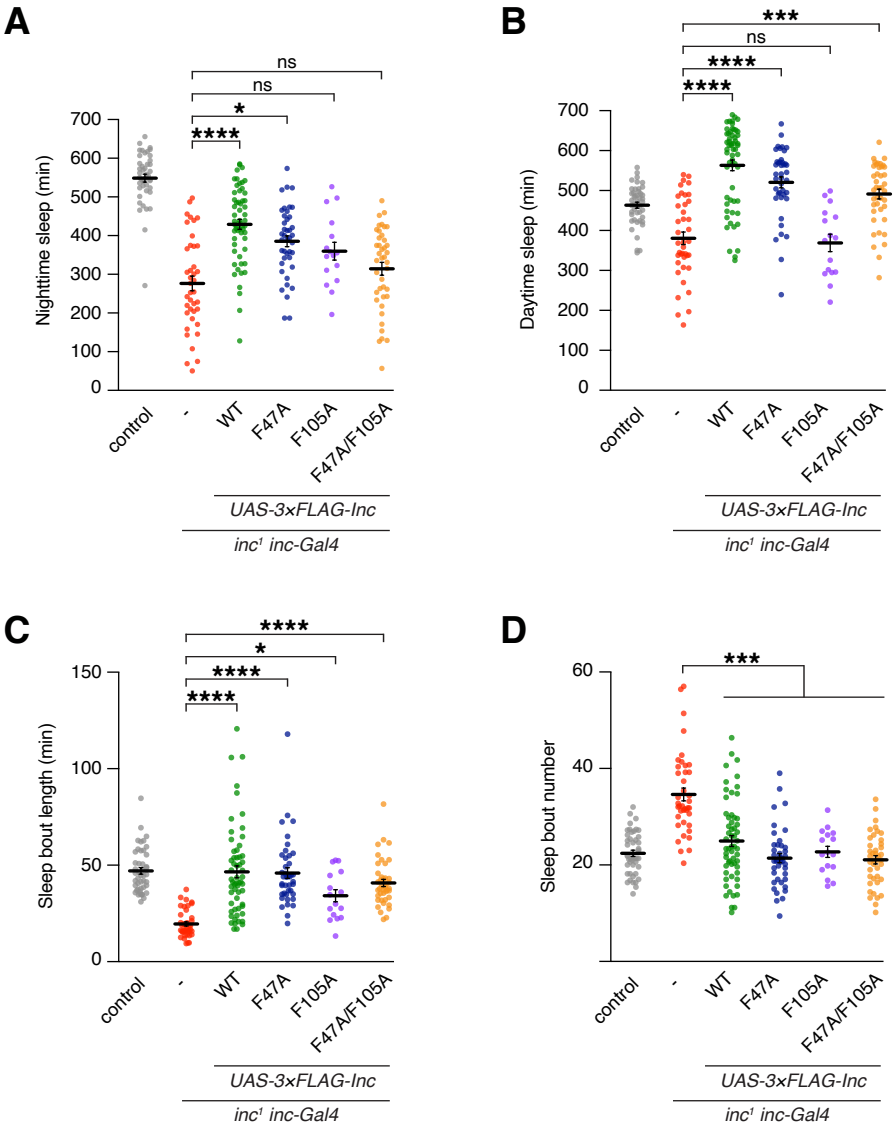

Supplementary Figure 7

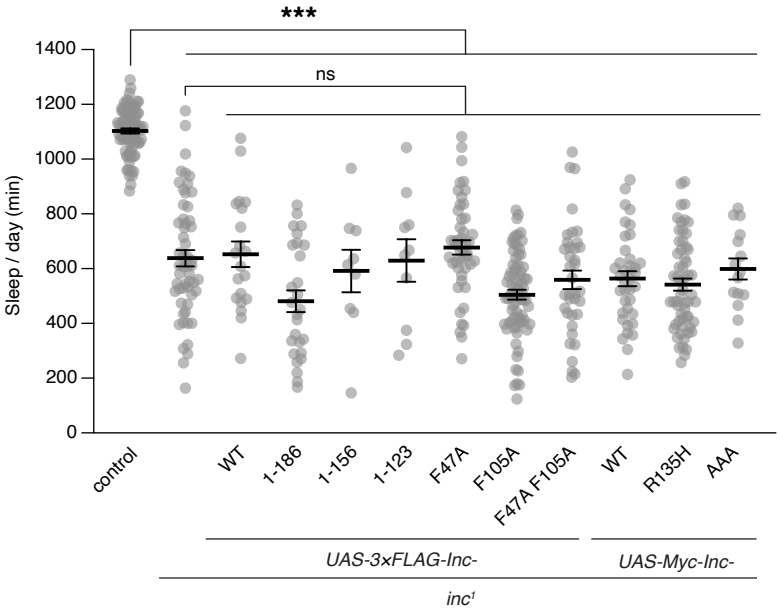

Supplementary Figure 8

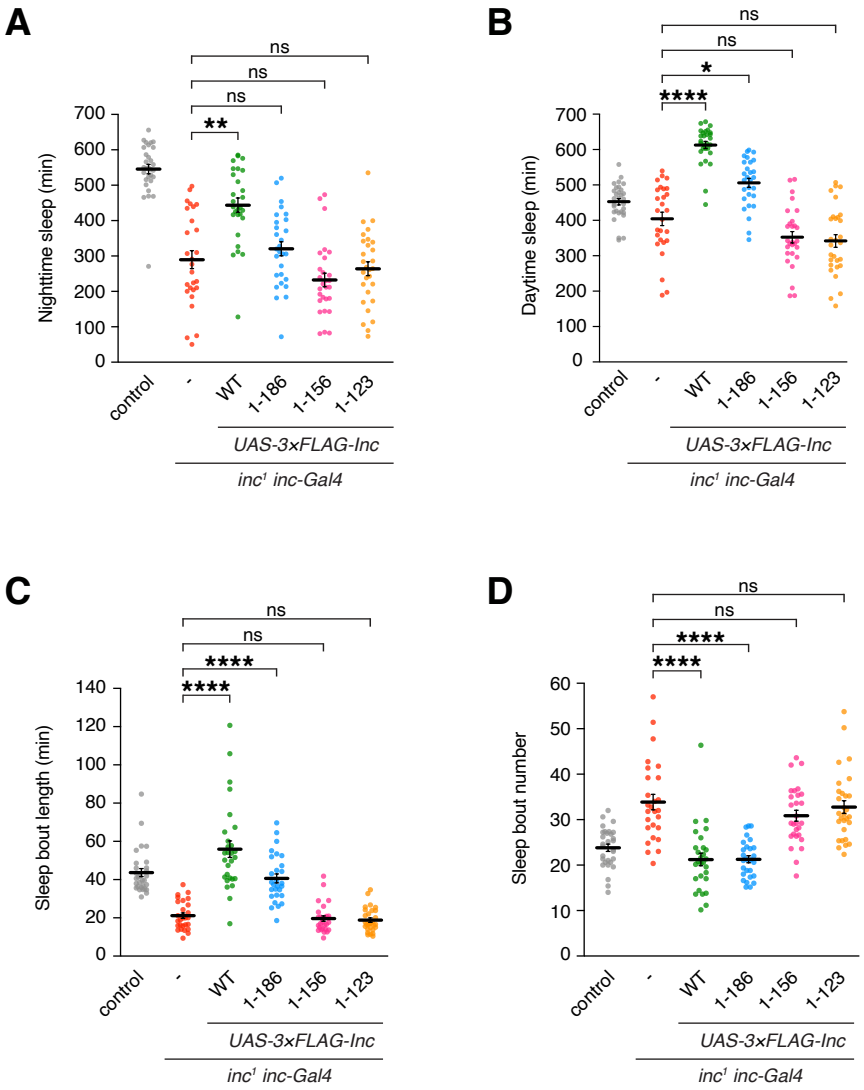

Supplementary Figure 9

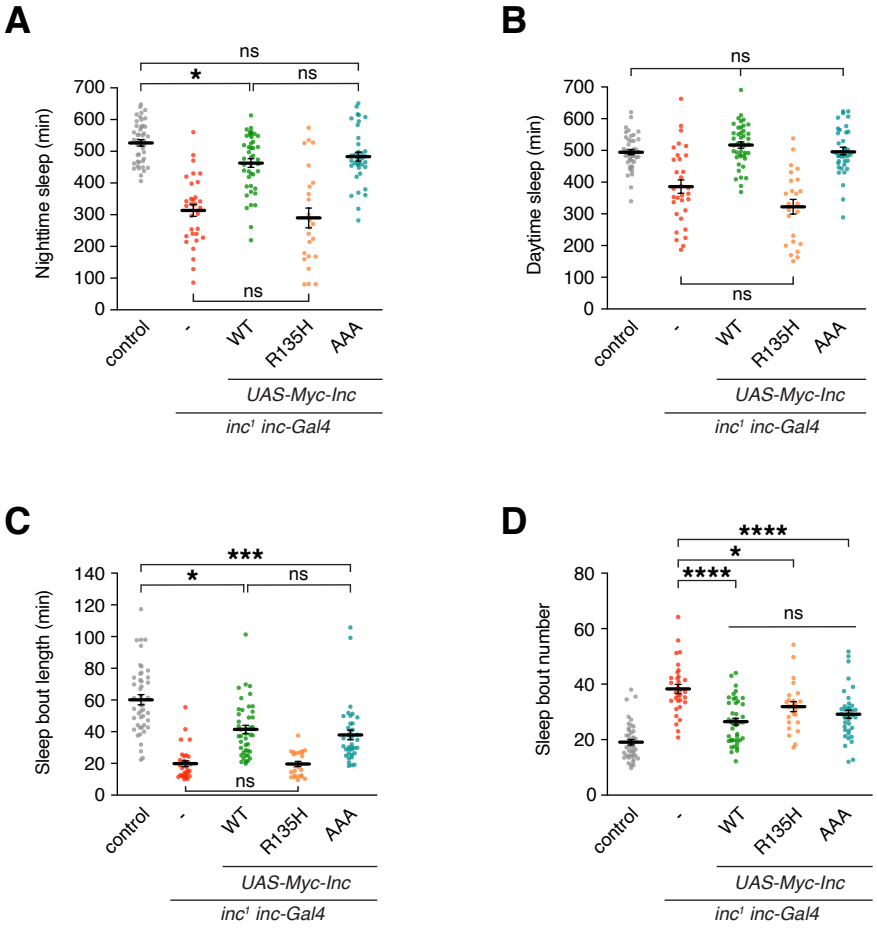

Supplementary Figure 10